A Series of Substituted Bis-Aminotriazines Are Activators of the Natriuretic Peptide Receptor C

Robert J. Smith,[§] Cristina Perez-Ternero,[§] Daniel Conole, Capucine Martin, Samuel H. Myers, Adrian J. Hobbs,* and David L. Selwood*

Cite This: *J. Med. Chem.* 2022, 65, 5495−5513

Read Online

ACCESS | Metrics & More | Article Recommendations | Supporting Information

ABSTRACT: C-type natriuretic peptide (CNP) is involved in the regulation of vascular homeostasis, which is at least partly mediated through agonism of natriuretic peptide receptor C (NPR-C), and loss of this signaling has been associated with vascular dysfunction. As such, NPR-C is a novel therapeutic target to treat cardiovascular diseases. A series of novel small molecules have been designed and synthesized, and their structure−activity relationships were evaluated by a surface plasmon resonance binding assay. The biological activity of hit compounds was confirmed through organ bath assays measuring vascular relaxation and inhibition of cAMP production, which was shown to be linked to its NPR-C activity. Lead compound **1** was identified as a potent agonist ($EC_{50} \sim 1\ \mu M$) with promising *in vivo* pharmacokinetic properties.
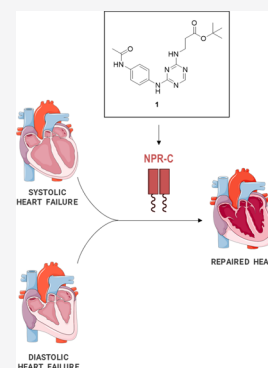
INTRODUCTION

The natriuretic peptide receptors (NPR) are a class of transmembrane receptors found in several tissues including the brain, bone, vascular and cardiac tissue, and are divided into three known isoforms, NPR-A, NPR-B, and NPR-C.[1,2] NPR-A and NPR-B are coupled to a guanylyl cyclase domain, and upon ligand binding, the levels of cyclic GMP are increased.[3,4] NPR-A is the cognate receptor for atrial natriuretic peptide (ANP) and brain natriuretic peptide (BNP), and cardiac-derived hormones that have been well characterized to regulate cardiovascular homeostasis. NPR-C is also a transmembrane protein; however, unlike NPR-A and NPR-B, it lacks the guanylyl cyclase domain; instead, it is a G-protein-coupled receptor that modulates adenylyl cyclase, phospholipase Cβ, and G-protein-coupled inwardly rectifying potassium channels, the latter of which produces vascular smooth muscle relaxation.[5,6] In addition to this activity, NPR-C also mediates a variety of other cardioprotective effects including antiplatelet, antileukocyte, antihyperthrombotic, and antithrombotic activities.[7] NPR-C has received significantly less attention than either NPR-A or NPR-B, in part as this receptor was initially classified simply as a clearance receptor.[8] However, recent studies have demonstrated that NPR-C has defined biological functions including a critical role in the regulation and maintenance of cardiovascular homeostasis, and loss of this signaling is associated with hypertension, cardiac hypertrophy/fibrosis, increased atheroma formation, and aneurysm in mouse models.[7,9,10] As such, the natriuretic peptide receptors are potentially a new therapeutic target to treat cardiovascular diseases.

The natriuretic peptides ANP, BNP, and CNP (**2−4**) are the natural ligands for the NPR receptors and bind with varying specificities to the different receptor types (Figure 1).[11] Several synthetic peptides that bind to these receptors have been developed, such as TAK-639 for NPR-B,[12] the truncated natriuretic peptide cANF[4−23] (**5**),[8] and the agonist PL-3994 (**7**), which are a selective NPR-C agonist and NPR-A agonists, respectively.[13] A chimeric peptide approach has also yielded some success, producing the chimeric CD-NP (**6**), a fusion of the active CNP and part of the *Dendroapsis* natriuretic peptide, with an improved *in vivo* profile compared to the natural ligands.[14]

Peptidomimetic small molecules that exhibit binding to the natriuretic peptide receptors have been developed, such as the antagonist M372049 (**8**, Figure 2).[15,16]

In 2008, a series of triazine-based compounds acting as NPR-A agonists were disclosed in a patent (**9−10**, Figure 3),[17] and in 2017, a series of three papers expanded upon this work and disclosed a second series of NPR-A agonists with selectivity optimized for human and rat NPR-A, with *in vitro* and *in vivo* activity (**11−12**); however, the method of NPR-A activation was not disclosed in these publications and no binding data of these compounds for NPR-A or other NPRs

ANP (2)

H-SLRRSSCFGGRMDRIGAQSGLGCNSFRY-OH

BNP (3)

H-SPKMVQGSCFGRKMDRISSSSGLGCKVLRR-OH

CNP (4)

H-DLRVDTKSRAAWARLLQEHPNARKYKGANKK GLSKGCFGLKLDRIGSMSGLGC-OH

cANF^4-23 (5)

H-RSSCFGGRMDRIGACN-OH

CD-NP (6)

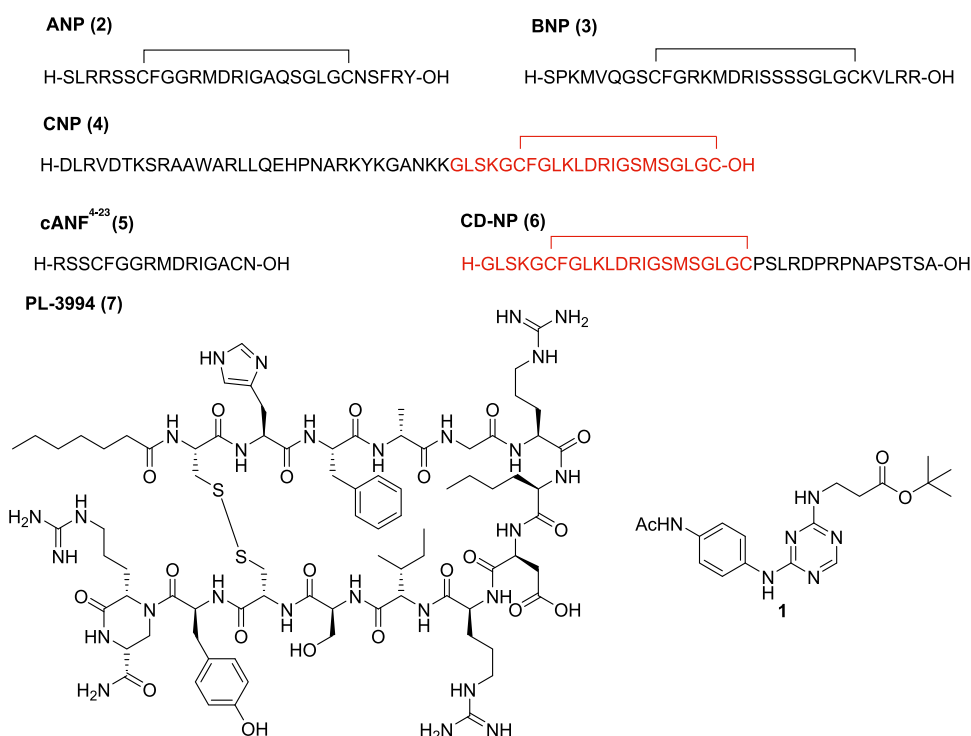H-GLSKGCFGLKLDRIGSMSGLGCPSLRDPRPNAPSTSA-OH
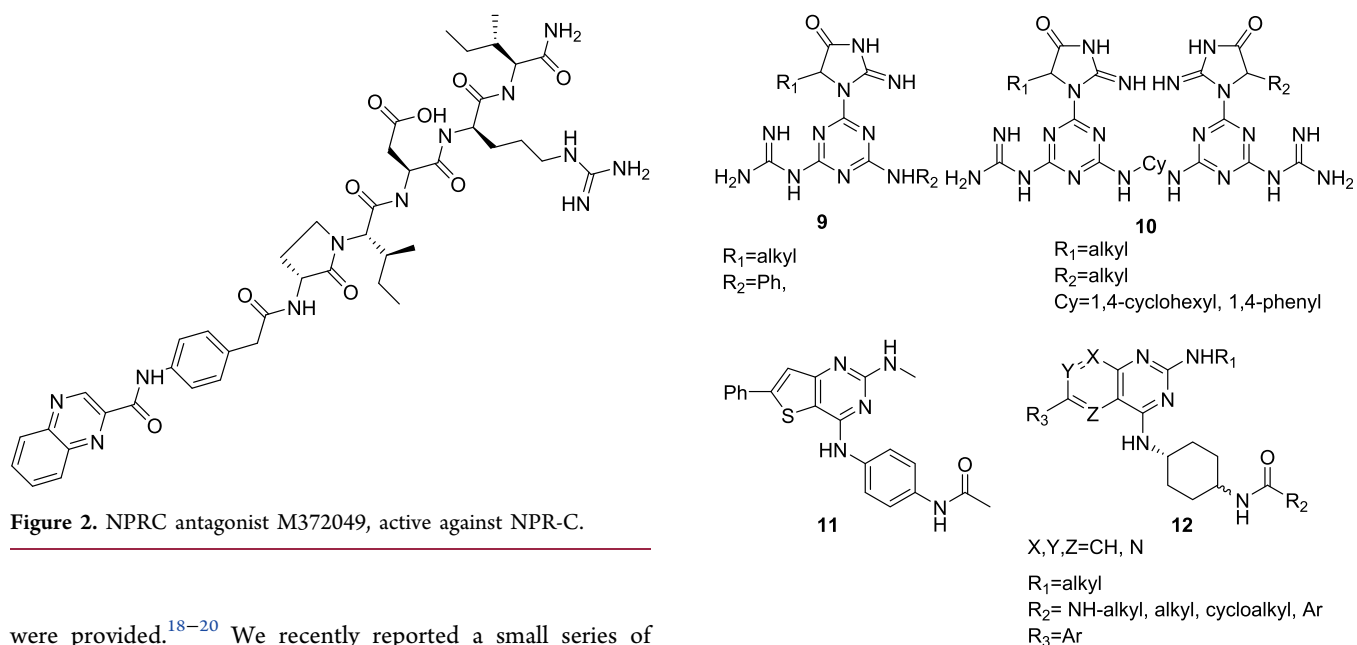
PL-3994 (7)

Figure 1. Structures of NPR-C active peptides and lead compound **1**; active CNP peptide are displayed in red, and brackets denote disulfide bonds.


Figure 2. NPRC antagonist M372049, active against NPR-C.

9

R$_1$=alkyl
R$_2$=Ph,

10

R$_1$=alkyl
R$_2$=alkyl
Cy=1,4-cyclohexyl, 1,4-phenyl

11

12

X,Y,Z=CH, N

R$_1$=alkyl
R$_2$= NH-alkyl, alkyl, cycloalkyl, Ar
R$_3$=Ar

13

Figure 3. Small molecule NPR-A and NPR-C agonists.

were provided.[18−20] We recently reported a small series of NPR-C agonists with low micromolar potency in *in vitro* and *in vivo* models, exemplified by the lead compound **13** depicted in Figure 3.[7]

We are interested in the potential of NPR-C agonists as potential treatments for heart failure and myocardial infarction. A small-molecule agonist would be an ideal drug candidate as an alternative to the natural cyclic peptide ligands, which have significant challenges in both production and delivery to achieve a clinical effect.

Herein, we report the development of a new series of small-molecule agonists for the NPR-C receptor. A detailed study of the structure−activity relationships (SAR) and evaluation of pharmacokinetic parameters of key compounds was undertaken, which allowed identification of **1** with potent *in vitro*

biological activity and promising *in vitro* and *in vivo* drug metabolism and pharmacokinetic (DMPK) data.

Scheme 1. Synthesis of 1,4-Cyclohexane Disubstituted Bis-Triazine and Monomeric Chlorotriazine Derivatives
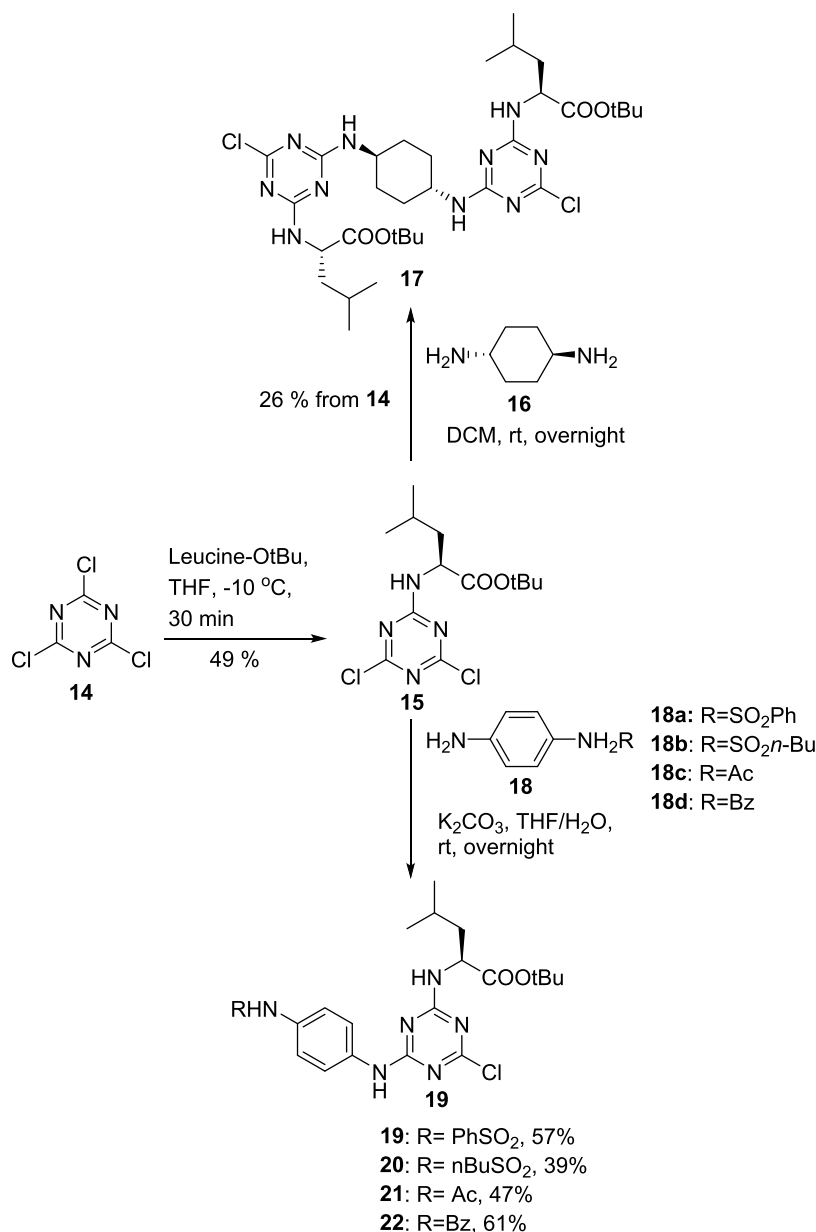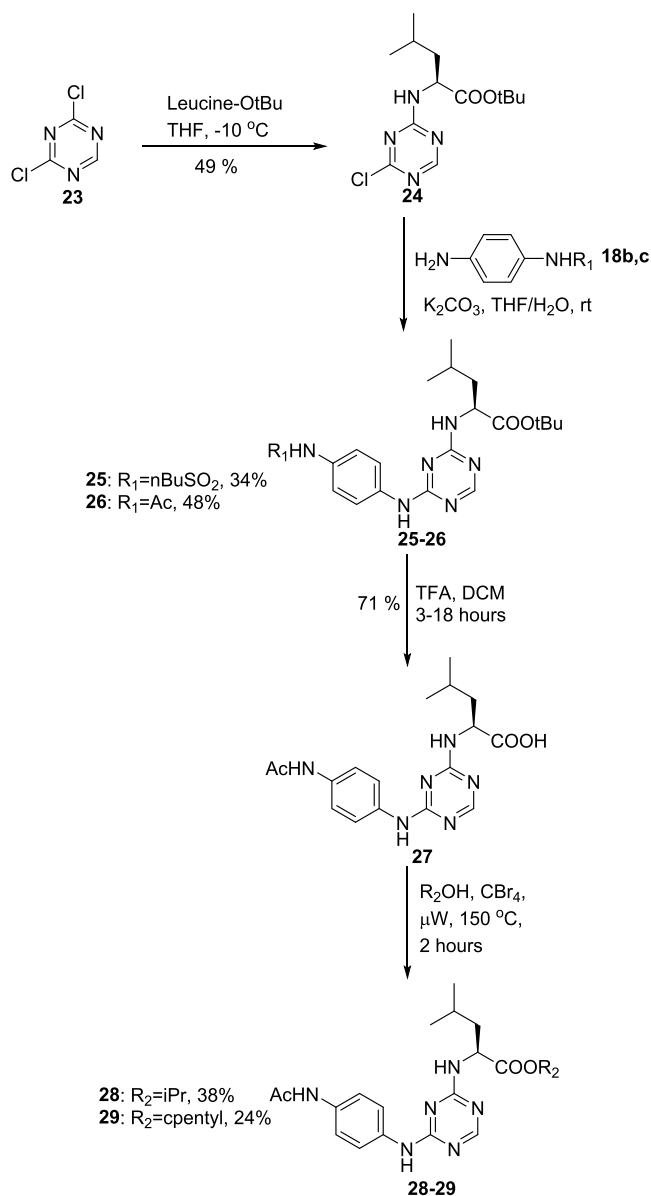

RESULTS AND DISCUSSION

Design of NRPC Agonists. A patent filed in 2008 reported several triazine-based scaffolds (Figure 3) capable of NPR-A agonism.[17] Given that the NPR-A and NPR-C receptors bind the same natural ligands and there was no reported selectivity data for these scaffolds, the core motifs were considered a potential starting point for the development of a series of NPR-C agonists. The reported molecules were notably non-drug-like, and in the first instance, we opted to both simplify the synthesis and probe structure–activity relationships. It was decided not to install the guanidino functionalities but to leave the acyclic amino acid group, which was a successful motif in the previous small-molecule agonists we prepared.[7]

Chemistry. Synthesis of the initial series of analogues proceeded by adapting established chemistry for the substitution of chlorotriazine derivatives,[19] and the treatment of 1,3,5-trichlorotriazine (14) with the *tert*-butyl ester of leucine at −10 °C in tetrahydrofuran (THF) formed the

nucleophilic aromatic substitution adduct 15, which underwent dimerization with *trans*-1,4-diaminocyclohexane in a one-pot process to provide 17 (Scheme 1). Several truncated analogues 19–22 were also prepared from 14 in two steps and in moderate yields by treatment of 15 with potassium carbonate in a mixture of THF/water with the *p*-phenylenediamine-derived subunits (18a–d) with different capping groups to probe whether dimerization was necessary. The moderate yields were consistent with those previously obtained in the literature for similar transformations.[19]

Further analogues of 19 without the additional chlorine atom were prepared from dichlorotriazine (23) by sequential nucleophilic aromatic substitution with leucine *tert*-butyl ester and substituted phenylenediamine subunits to afford 25–26 in moderate yields using the methods previously described (Scheme 2). Yields compared favorably to similar transformations in the literature, which show significant variance, particularly for the second substitution step (from 5 to >95%),
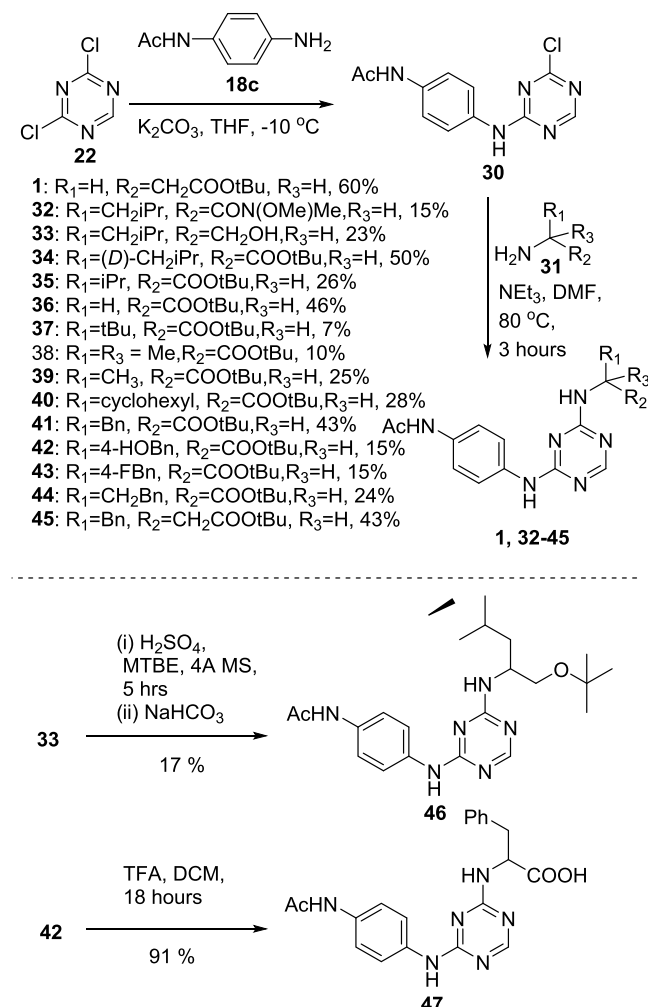
Scheme 2. Synthesis of L-Valine Triazine Derivatives

25: R₁=nBuSO₂, 34%
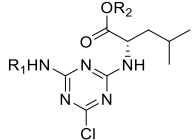**26**: R₁=Ac, 48%

28: R₂=iPr, 38%
29: R₂=cpentyl, 24%

Scheme 3. Synthesis of Amino Acid-Substituted Triazines

1: R₁=H, R₂=CH₂COOtBu, R₃=H, 60%
32: R₁=CH₂iPr, R₂=CON(OMe)Me,R₃=H, 15%
33: R₁=CH₂iPr, R₂=CH₂OH,R₃=H, 23%
34: R₁=(D)-CH₂iPr, R₂=COOtBu,R₃=H, 50%
35: R₁=iPr, R₂=COOtBu,R₃=H, 26%
36: R₁=H, R₂=COOtBu,R₃=H, 46%
37: R₁=tBu, R₂=COOtBu,R₃=H, 7%
38: R₁=R₃ = Me,R₂=COOtBu, 10%
39: R₁=CH₃, R₂=COOtBu,R₃=H, 25%
40: R₁=cyclohexyl, R₂=COOtBu,R₃=H, 28%
41: R₁=Bn, R₂=COOtBu,R₃=H, 43%
42: R₁=4-HOBn, R₂=COOtBu,R₃=H, 15%
43: R₁=4-FBn, R₂=COOtBu,R₃=H, 15%
44: R₁=CH₂Bn, R₂=COOtBu,R₃=H, 24%
45: R₁=Bn, R₂=CH₂COOtBu, R₃=H, 43%

although sulfoxide and sulfonamide derivatives were typically associated with lower yields.[21−28] Removal of the *t*-butyl ester was performed under standard acid hydrolysis reaction conditions to provide **27**,[29] and a series of ester derivatives were prepared using procedures adapted from the literature to afford **28−29** in moderate yields.[30]

The synthesis of derivatives with different amino acids followed the previously established chemistry; starting from 2,3-dichlorotriazine (**20**), the common intermediate **30** was prepared through nucleophilic aromatic substitution (Scheme 3). A second nucleophilic aromatic substitution was performed at elevated temperatures to shorten the reaction time (3 h at 80 °C, cf. overnight at room temperature) to afford **1, 32−45** in low to moderate yields. Lower yields were typically obtained for molecules with complex functionality (e.g., free OH; **33**, **42**, labile amide; **32**), and shorter, sterically demanding side chains (**35**, **37**, **38**, **40**) for the former stability issues could explain the lowered yields. Alkylation of **33** using an SN1-type substitution afforded the *t*-butyl ether **46** in 17% yield and
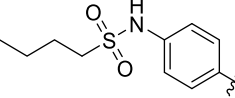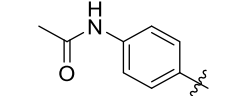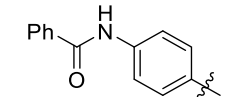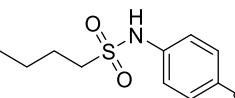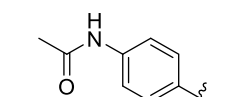
acid-promoted hydrolysis of **41** provided the phenylalanine acid derivative **47** in a high yield.

Biological Evaluation. At the outset of this study, we faced the challenge of how to assemble meaningful structure−activity relationships with only a low-throughput functional pharmacological assay in isolated blood vessels available for the determination of agonism. To address this issue, we developed two orthogonal binding assays for NPR-C using the extracellular domains of the receptor, a surface plasmon resonance assay using conventional amide coupling of the protein to a dextran-coated chip and a fluorescence polarization assay based on the displacement of a fluorescent NPR-C binding peptide, which has been reported elsewhere.[31] While binding is not necessarily related to agonism "*Corpora non agunt nisi fixate*", it allowed us to triage the compounds for affinity and active site occupancy and then to follow up with detailed organ bath and cell-based studies for agonism.

Binding Evaluation Using Surface Plasmon Resonance. Binding of these compounds to NPR-C was evaluated by surface plasmon resonance (SPR); in the first instance, a binding analysis is used to validate analyte binding, whereupon a full kinetic affinity assay is performed to calculate accurate K_D values using the affinity method. Molecules that displayed a very low response (<20% at 60 μM) in the binding assay and those with an R_{max} value much greater than the theoretical

Table 1. Effect of Changes to the Aryl and Cycloalkyl Groups on NPR-C Binding[a]

Compound	R_1	R_2	K_D (μM)[a]
17		CH_3	95.7±1.7
19		tBu	99±52
20		tBu	25.7±6.9
21		tBu	36.9 ±1.6
22		tBu	R_{max}>>theoretical
25		tBu	45.1 ±1.9
26		tBu	30.8±1.3

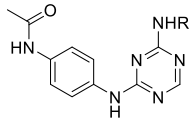[a]The SPR experiments were repeated with similar results.

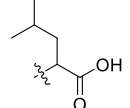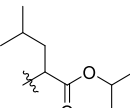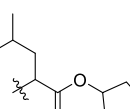maximum were not taken on for further testing, as these are signs of nonspecific/weak binding.
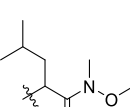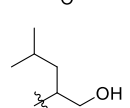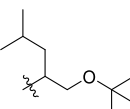
Analysis of the SPR data revealed that **17** bound with a moderate K_D of 95.7 ± 1.7 μM (Table 1). The binding of the truncated analogues compared favorably to this, with **19** binding with a similar K_D value of 99 ± 52 μM, while the alkylthioamide and acetamide-capped analogues **20** and **21** displayed more potent binding than the dimeric **17**, with K_D values of 25.7 ± 6.9 and 36.9 ± 1.6 μM, respectively. The benzamide derivative **22** displayed a poor binding profile in the initial SPR screen and was not taken on for full characterization. The *des*-chloro analogues **25** and **26** of the monomeric compounds were found to bind with a similar level of potency (K_D = 45.1 ± 1.9 and 30.8 ± 1.3 μM, respectively) to the chlorinated derivatives. Compound **26** with the acetamide capping group was selected as a potential lead compound for further development and analysis of structure−activity relationships.

Next, the effect of the amino acid ester on the SAR was investigated (Table 2). The leucine-free acid analogue **27** resulted in significantly reduced potency in the SPR experiment, with a K_D of 220 ± 22 μM. The isopropyl ester analogue **28** likewise displayed less potent binding (K_D 84.4 ± 2.8 μM), and interestingly, the cyclopentyl ester **29** retained the binding

potency (K_D 25.0 ± 3.1 μM) with a slight improvement over **26**. Removal of the ester carbonyl to furnish the *t*-butyl ether analogue **46** maintained comparable binding potency (K_D 42.2 ± 9.6 μM), while the alcohol analogue **33** suffered a significant reduction in potency (K_D 163 ± 6.1 μM), which indicated that the nonpolar functionality was more important than possible hydrogen-bonding interactions of the carbonyl. The Weinreb amide **32** likewise reduced the potency of binding with a K_D of 144 ± 7.7 μM. This information would suggest that the ester group is located near a nonpolar binding pocket and that the ester carbonyl may be involved in a minor stabilizing interaction (H-bonding), which is lost upon reduction of the carbonyl to the alcohol or ether. While the cyclopentyl ester **29** has a slightly increased potency compared to the *t*-butyl ester of **26**, given the commercial availability of precursors and shorter synthetic route, the *t*-butyl ester motif was retained for future analogues.

With SAR around the ester in hand, it was desired to examine the effect of the amino acid R group (Table 3). To determine the optimal geometry at the stereocenter, the D-leucine derivative **34** was prepared and had reduced potency compared to the lead **26**, failing to pass the preliminary binding screen for full SPR analysis. The valine analogue **35** with a shorter isopropyl side chain also resulted in a decreased
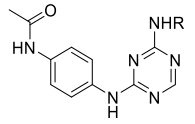
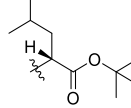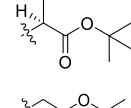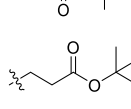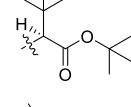**Table 2. Exploration of Binding Affinity with Variations to the Ester Group**[a]
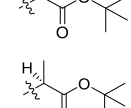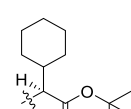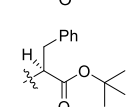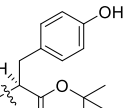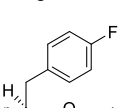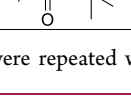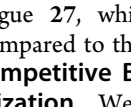
Compound	R	K_D (μM)[a]
27		220±22
28		84.4±2.8
29		25.0±3.1
32		144±7.7
33		163±6.1
46		42.2±9.6

[a]The SPR experiments were repeated with similar results.

Table 3. Exploration of Binding Affinity for Different Amino Acid Analogues[a]
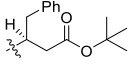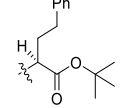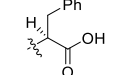
Compound	R	K_D (μM)[a]
34		Rmax<20%
35		79±47
36		832±190
1		146±39
37		201±6.1
38		Rmax<20%
39		Rmax<20%
40		28.0±4.9
41		31.3±7.3
42		Rmax<20%
43		23.7±3.8

[a]The SPR experiments were repeated with similar results.

binding potency in the SPR assay (K_D 79 ± 47 μM). The glycine (36), β-alanine (1) and t-butyl (37) derivatives displayed a loss of binding potency with K_D values over 100 μM. The dimethylalanine and alanine analogues 38−39 did not meet the minimum binding threshold to receive full SPR analysis. From these results, larger and smaller acyclic aliphatic chains and no side chain were found to be detrimental to binding activity. In contrast, cyclic aliphatic side chains such as that in 40 retained the binding potency compared to 26, with a K_D of 28.0 ± 4.9 μM. The phenylalanine analogue 41 retained the binding potency of the lead compound 26 with a K_D 31.3 ± 7.3 μM, as did the electron-deficient 4-fluorophenylalanine analogue 43 (K_D 23.73 ± 3.8 μM). It should be noted that the tyrosine analogue 42 did not meet the minimum binding threshold for full SPR analysis.

Further exploration of the phenylalanine analogue SARs was warranted due to potent binding in the SPR assay (Table 4). To this end, the effect of chain extensions of both the ester and benzyl portion of the molecule, analogues 44 and 45, respectively, was examined; both retained binding potency with K_D values of 29.6 ± 4.5 μM and 23.8 ± 2.0 μM, respectively. The free acid analogue 47 did not have a detectable change in binding potency (K_D 38 ± 17 μM) compared to 41; however, this is an improvement over the

valine-free acid analogue 27, which suffered a substantial decrease in potency compared to the lead t-butyl analogue 26.

Exploration of Competitive Binding to NPR-C Using Fluorescence Polarization. We previously developed a fluorescence polarization assay for the NPR-C extracellular domains.[31] This allowed us to determine if our compounds displaced a fluorescently labeled agonist peptide from the agonist binding region. Selected analogues were evaluated in this assay (Table 5). Analogues 26 and 44 were inactive in this assay, and 40 displayed a substantially lower response in this

Table 4. Exploration of Phenylalanine SAR[a]

Compound	R	K_D (µM)[a]
44		29.6±4.5
45		23.8±2.0
47		38±17
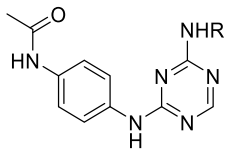
[a]The SPR experiments were repeated with similar results.

assay compared to the SPR result. In a primary screen for binding activity, analogue 1 displayed minimal activity in this assay with low binding (<17%) at 300 µM, and was not subjected to a full concentration-response assay as a result. Analogues 41 and 47 displayed comparable potency to the SPR assay. While the competition data do not mirror the SPR

results, it indicates that molecules from this series act on the NPR-C receptor at the same site as the peptide agonists.

NPR-C Agonist Activity and Selectivity in Organ Bath Studies. The vasodilatory effect of promising molecules as identified from SPR and competitive binding data was evaluated against both mouse small mesenteric artery (SMA) and rat aorta models (Table 6). When run with appropriate controls and challenged with specific antagonists, these assays provide measures of NPR-C agonist activity in separate rodent species; at the time of writing, there are no published data showing that NPR-C causes vasorelaxation in the rat aorta.[7] Selective NPR-C agonism in rat aorta (Figure 4A) and SMA (Figure 4B) was confirmed by the complete inhibition of cANF[4−23]-induced vasodilatation in the presence of the antagonists M372049 or osteocrin. Dimeric compound 17 displayed low micromolar EC_{50} values, in both rat SMA (0.97 ± 1.17 µM) and aorta (1.43 ± 3.06 µM). Analogues 40 and 43 had similar micromolar potency (6.24 ± 12.87 and 4.43 ± 2.36 µM, respectively) in rat aorta. The acid analogue 27 displayed a higher potency in the rat aorta than in SMA, while compound 39 was significantly more potent in rat SMA. β-Alanine analogue 1 displayed submicromolar activity in rat SMA (0.86 ± 0.23 µM) but was less potent in the rat aorta (15.51 ± 4.00 µM). Phenylalanine analogue 41 retained potency (0.39 ± 0.08 µM) in the mouse SMA, but it was substantially less potent in the rat aorta (>100 µM). Interestingly, the chain-extended phenylalanine analogues 44

Table 5. Competitive Binding of Selected NPR-C Agonists
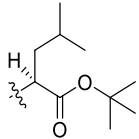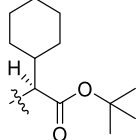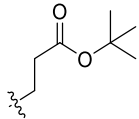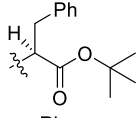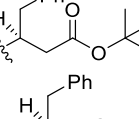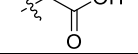
Compound	R	FP EC_{50} (µM)	SPR K_D (µM)
26		Inactive	30.8±1.9
40		326.7±12.3	28.0±4.9
1		Low % binding	146±39
41		32±15	31.3±7.3
44		Inactive	29.6±4.5
47		60±10	38±17

Table 6. NPR-C Agonist Evaluation in Small Mesenteric Artery and Rat Aorta[a]

Compound	Structure	Rat small mesenteric artery		Rat aorta	Mouse small mesenteric artery	
		EC_{50} (μM) ± SEM (μM)	EC_{50}+NPR-C inhibitor (M372049) ± SEM (μM)	EC_{50} ± SEM (μM)	WT EC_{50} ± SEM (μM)	NPR-C KO EC_{50} ± SEM (μM)
17		0.97 ± 1.17 (n=4)	0.47 ± 0.68 (n=3) (P=0.2518)	1.43 ± 3.06 (n=4)	1.16 ± 0.89 (n=4)	2.64 ± 1.10 (n=3) (P=0.9668)
27		22.18 ± 34.61 (n=3)	n.t.	6.20 ± 9.72 (n=3)	n.t.	n.t.
1		0.86 ± 0.23 (n=7)	8.64 ± 1.96 (n=5) (****P<0.0001)	15.51 ± 4.00 (n=4)	1.58 ± 0.72 (n=4)	10.09 ± 12.9 (n=4) (**P=0.0013)
39		3.45 ± 6.33 (n=3)	n.t.	78.07 ± 0.58 (n=2)	n.t.	n.t.
40		n.t.	n.t.	6.24 ± 12.87 (n=4)	n.t.	n.t.
41		0.39 ± 0.08 (n=5)	0.36 ± 0.07 (n=3) (P=0.9027)	102.2 ± 1.80 (n=5)	2.51 ± 3.57 (n=5)	3.02 ± 0.51 (n=4) (P=0.7134)
43		n.t.	n.t.	4.43 ± 2.36 (n=4)	n.t.	n.t.
44		n.t.	n.t.	21.38 ± 11.00 (n=2)	n.t.	n.t.
45		n.t.	n.t.	3.76 ± 2.24 (n=4)	n.t.	n.t.

[a]P value was calculated by two-way ANOVA from full dose−response curves.

and 45 had improved potency (21.38 ± 11.00 and 3.76 ± 2.24 μM, respectively) in the rat aorta relative to 41 (>100 μM).

The structure−activity relationships derived from the SPR data largely hold true for these biological assays, with larger,
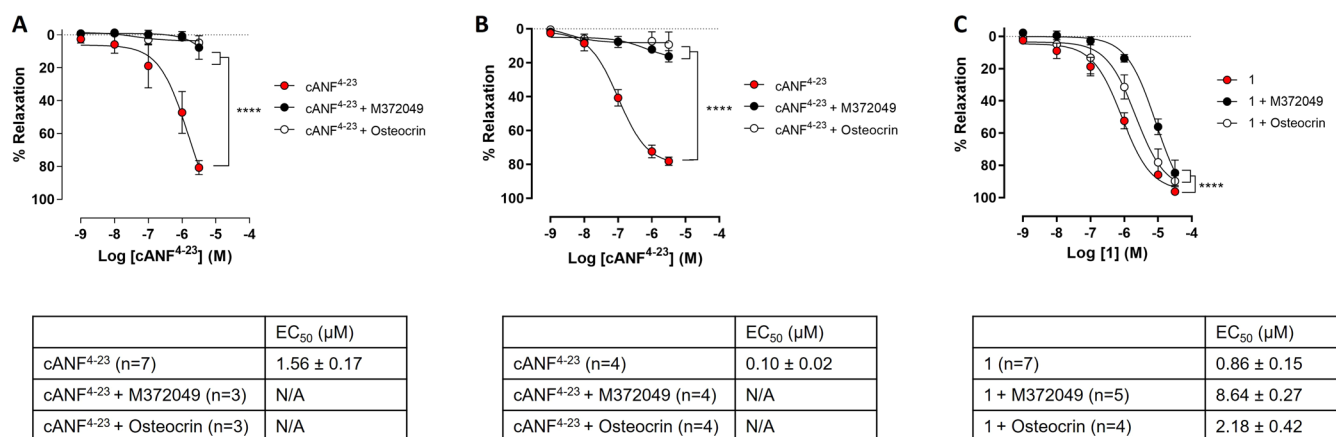
Figure 4. Reversal of agonist-induced vasorelaxation upon treatment with NPR-C inhibitors in rat aorta and small mesenteric artery. The selective NPR-C peptide agonist cANF$^{4-23}$ causes vasorelaxation that is blocked by M372049 and osteocrin in (A) rat aorta and (B) small mesenteric artery. (C) In rat small mesenteric artery small-molecule agonist **1** causes vasorelaxation that is partially blocked by M372049 and osteocrin.
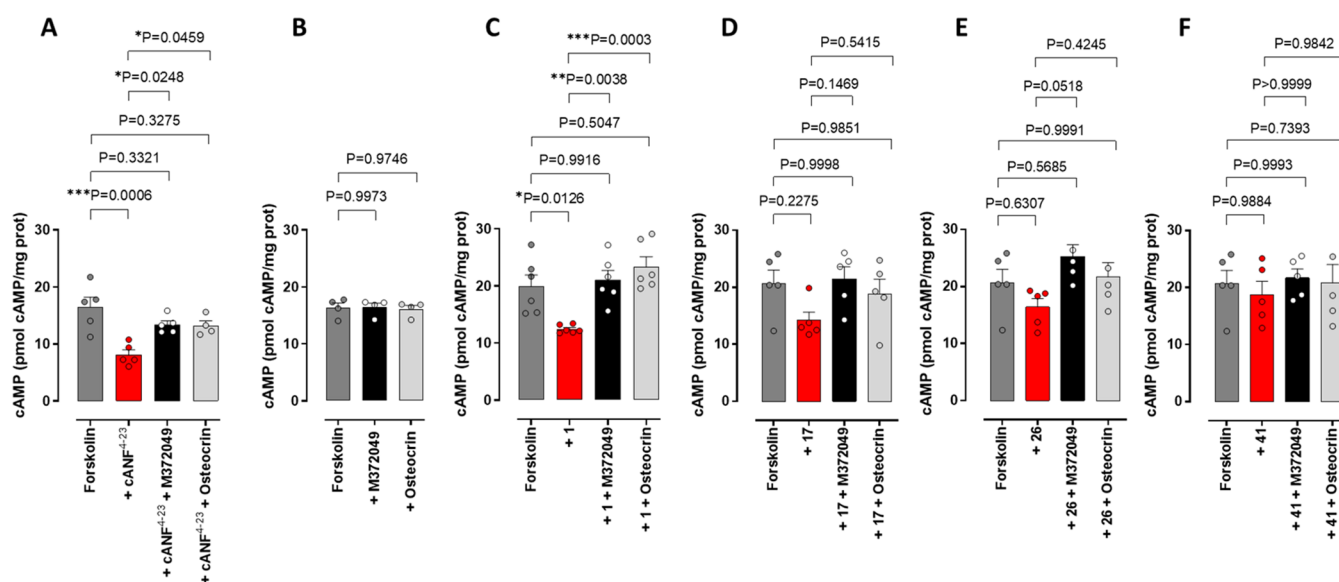
Figure 5. Evaluation of NPR-C agonism in HeLa cells by a cAMP assay. (A) cANF$^{4-23}$ (100 nM) inhibits cAMP formation and is reversed by M372049 (10 μM) and osteocrin (100 nM); (B) M372049 and osteocrin do not affect basal forskolin-induced cAMP production. Small-molecule agonists **1** (C), **17** (D), **26** (E), and **41** (F) (100 μM) inhibit cAMP formation by 37.67, 31.43, 20.65, and 9.16%, respectively, and is reversed by M372049 and osteocrin. Data points shown in the figures represent independent biological replicates.

nonpolar R-groups and esters eliciting a more potent response. However, there was a significant difference in potency between the mouse SMA and rat aorta, for most compounds tested (up to 3 orders of magnitude difference), which could not be fully accounted for.

The selectivity of these molecules to target NPR-C was also examined for several compounds using both rat SMA treated with a selective NPR-C antagonist (M372049 or osteocrin) and by comparison of SMA from wild-type and NPR-C knockout (KO) mice to validate that the observed biological effect could be attributed to NPR-C agonism. The positive control, selective NPR-C agonist cANF$^{4-23}$ effectively displayed a complete loss of vasorelaxant activity in rat aorta and rat small mesenteric artery (Figure 4A,B). Compound **1** showed between 2.5- and 10-fold reduction in potency (EC$_{50}$ value) when treated with osteocrin or M372049, respectively, in rat SMA (Figure 4C) and a 6.4-fold reduction in potency in NPR-C KO tissue, which was consistent with a loss of NPR-C signaling. However, this was not a complete inhibition of

vasodilation, which raised the question of off-target vasorelaxant activity. Compounds **17** and **41** maintained their activity in the presence of M372049 and in NPR-C KO small mesenteric artery despite showing a high receptor binding. These results indicate that while a portion of the biological activity is caused by NPR-C signaling, this series of compounds also exhibit some off-target activity contributing to the observed vasodilation, which complicates interpretation of structure–activity relationships. Indeed, if the EC$_{50}$ for the off-target pathway is lower than that for NPR-C, the inhibition with specific NPR-C antagonist or in KO tissue would be masked. Of note, higher off-target activity seemed to be associated with larger R groups (i.e., β-alanine compared to leucine or phenylalanine). Therefore, we developed other functional assays to assess NPR-C activation that were unaffected by the inherent vasorelaxation caused by these molecules (e.g., cAMP production, *vide infra*).

Human NPR-C Evaluation in HeLa Cells. Human HeLa cells express a functional NPR-C receptor and represent a
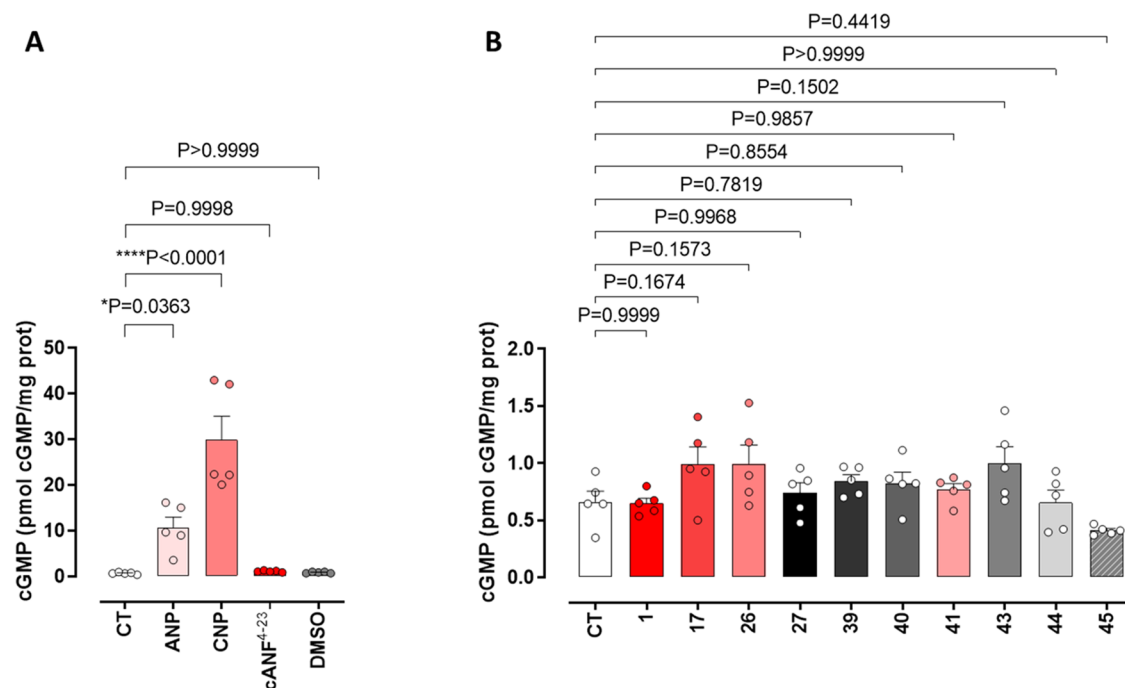
Figure 6. Human NPR-A and NPR-B agonism evaluation in HeLa cells. (A) ANP (1 μM) and CNP (1 μM) induce cGMP formation. (B) Selected compounds (10 μM) do not modify cGMP production. Data points shown in the figures represent independent biological replicates.

Table 7. Solubility, Permeability, and *In Vitro* Metabolism

			hepatocyte (rat)				
compound	solubility (mg/mL)	PAMPA P_{app} (cm/S $\times 10^{-6}$)	$T_{1/2}$ (min)	CL (μL/min/10^6)	human plasma $T_{1/2}$ (min)	plasma protein binding (% bound)	Cyp-P450 inhibition (IC$_{50}$ μM)
17	>122.52	<0.023	>216.8	<0.64	>60	99.5	2C9 (4.96)
							2C19 (37.8)
26	<0.414	6.07	12.2	113.7	>120	94.1	1A2 (26.8)
							2C8 (7.30)
							2C9 (30.6)
							2C19 (16.4)
							3A4-M (29.9)
							3A4-T (16.7)
41	11.61	7.35	6.0	230.4	>120	97.2	2C8 (7.72)
							2C9 (17.7)
							2C19 (14.7)
							3A4-M (19.8)
							3A4-T (11.6)
1	71.71	0.94	117.9	11.8	>120	71	all > 50
27	>71.68	<0.001	216.8	<6.4	>60	85.4	all > 50

useful direct way to determine NPR-C agonist activity through the measurement of an agonist-induced decrease of downstream cAMP levels.[6] We evaluated **1**, **17**, **26**, and **41** in this model and compared the response with the selective NPR-C agonist cANF[4−23]. cANF[4−23] (100 nM) caused a clear decrease in the cAMP levels induced with the adenylyl cyclase stimulator forskolin (10 μM), and this was reversed by the antagonists M372049 (10 μM) and osteocrin (100 nM) (Figure 5A). A similar reduction of cAMP was induced upon the addition of **1** (100 μM), and this was reversed by antagonist application (Figure 5C). Compounds **17** and **26** showed an inhibition trend that did not reach statistical significance. Compound **41** inhibited cAMP formation only minimally (9.16%), suggesting that despite binding NPR-C, it did not activate the receptor.

Human NPR-A and NPR-B Agonism Evaluation in HeLa Cells. To evaluate potential residual NPR-A or NPR-B agonism, we tested the ability of selected compounds to induce cGMP formation as a surrogated measurement for NPR-A and/or NPR-B activation. ANP (1 μM) and CNP (1 μM) caused an increase in cGMP formation as a result of NPR-A and NPR-B activation, respectively (Figure 6A). In contrast, neither the NPR-C specific agonist nor the vehicle (DMSO) induced any cGMP production, as expected (Figure 6A). None of the compounds tested caused an increase in intracellular cGMP, suggesting a lack of agonism for these receptors (Figure 6B).

Absorption, Distribution, Metabolism, and Excretion (ADME) Data. To evaluate potential candidates for future *in vivo* testing and to generate structure−activity relationships

around ADME for this series, several promising analogues with diverse structures were evaluated for ADME properties, and the data are presented in (Table 7). Solubility and membrane permeability assessed by parallel artificial membrane permeability assay (PAMPA) predictably displayed an inverse correlation, with the dimeric 17, free acid 27, and glycine derivative 36 lacking a nonpolar R group displayed a relatively high solubility of >70 mg/mL and a low membrane permeability ($<1 \times 10^{-6}$ cm/s), while the more nonpolar 26 and 41 were almost insoluble (0.414, 11.61 mg/mL), but have improved membrane permeability (6.07 and 7.35×10^{-6} cm/s respectively). The dimer 17 displayed a long half-life in rat hepatocytes (>200 min), which was also evident in human plasma (>60 min). However, both rat and human plasma were almost completely bound to plasma protein (>99.5%) and two CypP450 isoforms were inhibited (EC_{50} 4.96−37.8 μM). The more lipophilic 26 had a high clearance rate and consequently a low half-life in rat hepatocytes (12 min) but retained the long half-life in human plasma. There was also inhibition of a half-dozen CypP450 isoforms (EC_{50} 7.30−30.6 μM). Phenyl-alanine analogue 41 suffers from similar issues with a long half-life in human plasma (>120 min) but a high proportion (97.2%) bound to plasma proteins and a high clearance rate and consequently low half-life in rat hepatocytes and plasma (<10 min). Additionally, there was potentially problematic inhibition of five CypP450 isoforms (EC_{50} 7.72−19.8 μM). The β-alanine derivative 1 displayed more favorable properties, with decreased clearance and increased half-life in rat hepatocytes with a half-life of almost 2 h, a long half-life (>120 min) in human plasma, lower binding to plasma proteins (71%), and all CypP450 isoforms tested had inhibition $EC_{50} > 50$ μM. The free acid valine analogue 27, which substantially improves the pharmacokinetic properties compared to the *t*-butyl ester 26, had a half-life in rat hepatocytes of over 3 h and >60 min half-life in human plasma, with only 85% bound to plasma proteins and high EC_{50} (>50 μM) for all CypP450 isoforms tested.

The lipophilic analogues 26 and 41 with the highest potency in both SPR and biological assays performed the worst in terms of pharmacokinetic profiles, with the more polar analogues providing a better pharmacokinetic profile. Promisingly the leucine-free acid analogue 27 did not have the clearance or CypP450 inhibition issues of the *t*-butyl ester. While this analogue was substantially less potent than the *t*-butyl ester, the phenylalanine-free acid analogue 47 retained potency in the SPR assays and would be expected to follow the same pharmacokinetic trends displayed by the leucine analogues.

With these data in hand, 1 was selected for an *in vivo* bioavailability study, and the results are shown (Tables 8 and 9). Compound 1 displayed a promising profile with a low clearance of 112 mL/min/kg and >40% bioavailability.

CONCLUSIONS

We have designed and synthesized a series of NPR-C agonists based upon molecules reported to bind the related natriuretic peptide receptor A. These compounds were tested in several assays to establish structure−activity relationships, which identified several compounds as binding to the target receptor. The link between receptor binding and biological effect was confirmed by vasodilation assays carried out on SMA and rat aorta. However, control experiments revealed some off-target activity. Nevertheless, the loss of activity in cell-based assays in the presence of M372049 and/or osteocrin suggests robust

Table 8. Intravenous PK Profile of 1 after Dosing at 3 mg/kg (Mice)

PK parameters	mean IV SD
C_0 (ng/mL)	2328 ± 233
$T_{1/2}$ (h)	0.566 ± 0.293
Vd_{ss} (L/kg)	1.75 ± 0.121
Cl (mL/min/kg)	112 ± 10.1
AUC_{0-inf} (ng·h/mL)	448 ± 42.3
MRT_{0-inf} (h)	0.262 ± 0.0377

Table 9. Oral PK Profile of 1 after Dosing at 10 mg/kg (Mice)

PK parameters	mean PO SD
C_{max} (ng/mL)	612 ± 139
T_{max} (h)	0.250 ± 0.000
$T_{1/2}$ (h)	1.37 ± 0.567
AUC_{0-inf} (ng·h/mL)	653 ± 141
MRT_{0-inf} (h)	1.33 ± 0.209
bioavailability (%)	43.8

target engagement.[11,15,16] One molecule, 1, showed promising NPR-C agonism in humans, mice, and rats and demonstrated a favorable pharmacokinetic profile.

EXPERIMENTAL SECTION

Materials and Methods. Commercially available starting materials were used as supplied without further purification. Reactions were carried out in dry solvents (dichloromethane (DCM), *N*,*N*-dimethylformamide (DMF), THF, cyclobutanol, cyclopentanol, isopropanol) unless otherwise noted. Reactions were monitored by thin-layer chromatography (TLC) and an Agilent 6100 single quadrupole LC 1200 series mass spectrometer. Purification was carried out on either a Biotage Isolera one or Biotage Isolera four system, with either C18 or silica gel prepacked columns. ^{1}H and ^{13}C NMR data were recorded on a 600 MHz Bruker Avance III with a 5 mm helium-cooled cryoprobe. Chemical shifts for ^{1}H and ^{13}C spectra were referenced to residual solvent. Mass spectra were obtained on an Agilent 1200 liquid chromatography system connected to an Agilent 6100 single quadrupole mass spectrometer. High-resolution mass spectrometry-electrospray ionization (HRMS-ESI) data were obtained on an Agilent 1200 liquid chromatography system connected to an Agilent 6510 QTOF mass spectrometer. Purity was determined by liquid chromatography−mass spectrometry (LCMS) analysis and is >95% for all compounds unless otherwise stated.

Human full-length (FL) NPR-C (27−541)-10His-Flag (GenBank accession: NM_000908) and extracellular domain (ECD) NPR-C (27−481)-6His were purchased from Peak Proteins, U.K. The FP probe 5-carboxyfluorescein N-terminus-labeled GLSKG-[CFGRSLDRIGSLSGLGC]NS (P19) was purchased from Peptide Protein Research Ltd, U.K. (Peptidesynthetics).

PAINS Statement. All compounds tested in these assays (1, 17, 19, 20−22, 25−29, 32−47) were run through the computational PAINS checkers https://www.cbligand.org/PAINS/login.php. All structures passed this analysis, and no PAINS flags were indicated. In addition, the two assays detailed in Figures 4 and 5 show dose-dependent competitive inhibition of 1 with the known NPR-C antagonist M372049, which provides unambiguous evidence of target engagement.

Chemistry. Compounds 18a−d were prepared following established literature procedures.[32−34]

tert-Butyl 3-((4-((4-Acetamidophenyl)amino)-1,3,5-triazin-2-yl)-amino)propanoate (1). To a solution of 30 (100 mg, 0.379 mmol) and *t*-Bu β-alanine HCl (103 mg, 0.569 mmol) in dry DMF (2 mL) at r.t. was added triethylamine (0.133 mL, 0.948 mmol), and the mixture was stirred at 80 °C for 3 h (TLC, LCMS). To the reaction was then

added water, and the resultant solid was filtered, washed with water, and then dried. Column chromatography (1:3, c-Hex, EtOAc) afforded the title compound as a white solid (0.085 g, 0.228 mmol, 60%).

^{1}H NMR (600 MHz, DMSO-d_6) δ/ppm: 9.81 (s, 1H), 9.45 (m, 1H), 8.15 (d, 1H, J = 65 Hz), 7.65 (d, 2H, J = 7.7 Hz), 7.49−7.44 (m, 2H), 3.48 (qn, 2H, J = 6.8 Hz), 2.01 (s, 3H), 1.39 (m, 9H).

^{13}C NMR (150 MHz, DMSO-d_6) δ/ppm: 170.6, 167.9, 165.8, 165.5, 164.9, 134.8, 134.1, 120.4, 119.3, 119.2, 79.9, 36.4, 35.1, 34.7, 27.8, 23.9.

LCMS [M + H] calcd for: $C_{18}H_{24}N_6O_3^+$ 373.19; measured 373.00.

Dimethyl 2,2′-(((((1r,4r)-Cyclohexane-1,4-diyl)bis(azanediyl))bis-(6-chloro-1,3,5-triazine-4,2-diyl))bis(azanediyl))bis(4-methylpenta-noate) (17). To L H-Leu-OMe (1.81 g, 10 mmol) and DIPEA (3.7 mL, 2.58 g, 20 mmol) in DCM (10 mL) at 0 °C was added cyanuric chloride (1.84 g, 10 mmol) as a solid in small portions, and the reaction was stirred at 0 °C for 30 min. Water (20 mL) was added, the reaction was stirred for 5 min, then the DCM was separated. To this mixture was added the *trans* diaminocyclohexane (0.98 g, 5 mmol) in DCM (5 mL), and the reaction was stirred overnight. The crude reaction mixture was purified directly by flash chromatography (Puriflash SiO$_2$, 40 g) using DCM/acetone gradient. This gave the product (0.88 g, 1.28 mmol) in 26% yield.

^{1}H NMR (400 MHz, DMSO, 70 °C) δ 7.89 (s, 1H), 7.61 (s, 1H), 4.48 (s, 1H), 4.39 (s, 1H), 3.69 (s, 2H), 3.65 (s, 6H), 1.90 (s, 4H), 1.72 (s, 4H), 1.59 (dq, J = 9.9, 5.1 Hz, 2H), 1.36 (s, 5H), 0.91 (dd, J = 12.3, 6.1 Hz, 12H).

HRESIMS [M + H] calcd for $C_{26}H_{50}N_{10}O_6Cl_2^+$, 627.2689; measured: 627.2692.

tert-Butyl (3-Chloro-5-((4-(phenylsulfonamido)phenyl)amino)-phenyl)-L-leucinate (19). To a stirred solution of **15** (30 mg, 0.09 mmol) in THF and water (5 mL, 0.5 mL) were added **18a** (22 mg, 0.09 mmol, 1 equiv) and potassium carbonate (19 mg, 0.18 mmol, 1.35 equiv). This was stirred at room temperature overnight. EtOAc and water (50 mL) were added to the mixture, and the organic layers were separated. The aqueous layer was washed with EtOAc (50 mL × 3), and the organic layers were combined and washed with water (30 mL × 2) and brine (20 mL), dried over anhydrous MgSO$_4$, and concentrated *in vacuo*. The crude product was purified by column chromatography MeOH/DCM (0−8%) to yield a beige solid (28 mg, 57% yield).

^{1}H NMR (600 MHz, chloroform-d) δ 7.74−7.73 (m, 1H), 7.73 (d, J = 1.5 Hz, 1H), 7.46 (d, J = 1.7 Hz, 2H), 7.45 (d, J = 2.1 Hz, 3H), 7.44 (d, J = 1.8 Hz, 1H), 7.03 (dd, J = 10.8, 8.8 Hz, 3H), 2.08 (d, J = 35.1 Hz, 1H), 1.71 (ddd, J = 19.4, 13.5, 6.2 Hz, 2H), 1.43 (d, J = 7.8 Hz, 9H), 1.28−1.24 (m, 1H), 0.97 (dd, J = 6.5, 4.7 Hz, 6H).

HRESIMS [M + H] calcd for $C_{25}H_{32}N_6O_4SCl^+$ 547.1889; measured: 547.1898.

tert-Butyl (4-((4-(Butylsulfonamido)phenyl)amino)-6-chloro-1,3,5-triazin-2-yl)-L-leucinate (20). To a stirred solution of **15** (50 mg, 0.1 5 mmol) in THF and water (5 mL, 0.5 mL) were added **18b** (34 mg, 0.15 mmol, 1 equiv) and potassium carbonate (31 mg, 0.22 mmol, 1.35 equiv). This was stirred at room temperature overnight. EtOAc and water (50 mL) were added to the mixture, and the organic layers were separated. The aqueous layer was washed with EtOAc (50 mL × 3), and the organic layers were combined and washed with water (30 mL × 2) and brine (20 mL), dried over anhydrous MgSO$_4$, and concentrated *in vacuo*. The crude product was purified by column chromatography MeOH/DCM (0−5%) to yield a pale yellow solid (30 mg, 39% yield).

^{1}H NMR (600 MHz, chloroform-d) δ 7.56−7.51 (m, 2H), 7.23−7.18 (m, 2H), 4.13 (q, J = 7.1 Hz, 1H), 3.10−3.06 (m, 2H), 2.18 (s, 2H), 1.49 (s, 4H), 1.46−1.40 (m, 9H), 1.25 (d, J = 4.1 Hz, 1H), 0.99 (d, J = 1.6 Hz, 2H), 0.98 (d, J = 1.5 Hz, 2H), 0.94−0.91 (m, 6H). ^{13}C NMR (151 MHz, CDCl$_3$) δ 132.57, 131.00, 128.92, 122.49, 122.27, 121.90, 82.40, 77.34, 77.13, 76.91, 68.28, 60.52, 53.11, 51.43, 41.91, 41.44, 31.05, 30.47, 29.04, 28.14, 28.10, 25.64, 25.05, 25.00, 23.86, 23.10, 23.00, 22.81, 22.31, 22.17, 21.56, 21.17, 14.32, 14.17, 13.68, 13.66, 11.08.

^{13}C NMR (151 MHz, CDCl$_3$) δ 132.57, 131.00, 128.92, 122.49, 122.27, 121.90, 82.40, 77.34, 77.13, 76.91, 68.28, 60.52, 53.11, 51.43, 41.91, 41.44, 31.05, 30.47, 29.04, 28.14, 28.10, 25.64, 25.05, 25.00, 23.86, 23.10, 23.00, 22.81, 22.31, 22.17, 21.56, 21.17, 14.32, 14.17, 13.68, 13.66, 11.08.

HRESIMS [M + H] calcd for $C_{23}H_{36}N_6O_4SCl^+$ 527.2202; measured: 527.2197.

tert-Butyl (4-((4-Acetamidophenyl)amino)-6-chloro-1,3,5-tria-zin-2-yl)-L-leucinate (21). To a stirred solution of **15** (56 mg, 0.167 mmol) in THF and water (5 mL, 0.5 mL) were added **18c** (25 mg, 0.167 mmol, 1 equiv) and potassium carbonate (35 mg, 0.2505 mmol, 1.35 equiv). This was stirred at room temperature for 5 h. EtOAc and water (50 mL) were added to the mixture, and the organic layers were separated. The aqueous layer was washed with EtOAc (50 mL × 3), and the organic layers were combined and washed with water (30 mL × 2) and brine (20 mL), dried over anhydrous MgSO$_4$, and concentrated *in vacuo*. The crude product was purified by column chromatography MeOH/DCM (0−8%) to yield a white solid (35 mg, 47% yield).

^{1}H NMR (600 MHz, chloroform-d) δ 7.50 (s, 2H), 7.48 (s, 1H), 7.12 (s, 2H), 2.19 (d, J = 1.9 Hz, 3H), 2.05 (s, 1H), 1.76−1.68 (m, 2H), 1.46 (d, J = 29.1 Hz, 9H), 1.26 (t, J = 7.1 Hz, 1H), 1.00−0.92 (m, 6H).

HRESIMS [M + H] calcd for $C_{21}H_{30}ClN_6O_3^+$ 449.1990; measured: 449.2062.

tert-Butyl (4-((4-Benzamidophenyl)amino)-6-chloro-1,3,5-tria-zin-2-yl)-L-leucinate (22). To a stirred solution of **15** (56 mg, 0.167 mmol) in THF and water (5 mL, 0.5 mL) were added **18d** (35 mg, 0.167 mmol, 1 equiv) and potassium carbonate (35 mg, 0.2505 mmol, 1.35 equiv). This was stirred at room temperature for 5 h. EtOAc and water (50 mL) were added to the mixture, and the organic layers were separated. The aqueous layer was washed with EtOAc (50 mL × 3), and the organic layers were combined and washed with water (30 mL × 2) and brine (20 mL), dried over anhydrous MgSO$_4$, and concentrated *in vacuo*. The crude product was purified by column chromatography MeOH/DCM (0−8%) to yield a yellow solid (52 mg, 61% yield).

^{1}H NMR (600 MHz, chloroform-d) δ 7.88 (dd, J = 8.4, 1.4 Hz, 2H), 7.81 (d, J = 5.2 Hz, 1H), 7.64 (dd, J = 13.2, 8.7 Hz, 2H), 7.57 (dd, J = 10.6, 3.5 Hz, 2H), 7.51 (td, J = 7.5, 1.8 Hz, 2H), 4.67−4.46 (m, 1H), 1.77−1.66 (m, 1H), 1.47 (d, J = 28.4 Hz, 9H), 1.32−1.20 (m, 1H), 1.00−0.92 (m, 6H), 0.90−0.80 (m, 1H).

HRESIMS [M + H] calcd for $C_{26}H_{32}N_6O_3Cl^+$ 511.2219; measured: 511.2206

tert-Butyl (4-Chloro-1,3,5-triazin-2-yl)-L-leucinate (24). L-Leucine *tert*-butyl ester hydrochloride was washed with sodium carbonate three times to yield L-leucine *tert*-butyl ester. A solution of 2,4-dichloro-1,3,5-triazine (250 mg, 1.67 mmol) in tetrahydrofuran (5 mL) was cooled to 10 °C by an ice-salt bath, and then L-leucine *tert*-butyl ester (372 mg, 1.67 mmol) in tetrahydrofuran (5 mL) was added slowly, and the mixture was stirred at room temperature for 30 min. EtOAc and water (50 mL) were added to the mixture, and the organic layers were separated. The aqueous layer was washed with EtOAc (50 mL × 3), and the organic layers were combined and washed with water (30 mL × 2) and brine (20 mL), dried over anhydrous MgSO$_4$, and concentrated *in vacuo*. The crude product was purified by column chromatography MeOH/DCM (0−10%) to give a white solid (279 mg, 49% yield).

tert-Butyl (4-((4-(Butylsulfonamido)phenyl)amino)-1,3,5-triazin-2-yl)-L-leucinate (25). To a stirred solution of **24** (50 mg, 0.167 mmol) in THF and water (5 mL, 0.5 mL) were added **18b** (40 mg, 0.15 mmol, 1 equiv) and potassium carbonate (31 mg, 0.22 mmol, 1.35 equiv). This was stirred at room temperature overnight. EtOAc and water (50 mL) were added to the mixture, and the organic layers were separated. The aqueous layer was washed with EtOAc (50 mL × 3), and the organic layers were combined and washed with water (30 mL × 2) and brine (20 mL), dried over anhydrous MgSO$_4$, and concentrated *in vacuo*. The crude product was purified by column chromatography MeOH/DCM (0−8%) to yield a yellow solid (29 mg, 34% yield).

^{1}H NMR (600 MHz, chloroform-*d*) δ 8.25 (d, *J* = 29.2 Hz, 1H), 7.71 (dd, *J* = 5.7, 3.3 Hz, 1H), 7.60−7.53 (m, 2H), 7.20 (dd, *J* = 8.7, 6.6 Hz, 1H), 6.21 (d, *J* = 3.9 Hz, 1H), 4.72−4.47 (m, 1H), 4.22 (qd, *J* = 10.9, 5.9 Hz, 2H), 3.09−3.05 (m, 2H), 2.98 (d, *J* = 43.5 Hz, 0H), 1.84−1.67 (m, 2H), 1.49−1.40 (m, 9H), 1.30 (d, *J* = 12.4 Hz, 2H), 1.01−0.94 (m, 3H), 0.95−0.88 (m, 6H).

HRESIMS [M + H] calcd for $C_{23}H_{37}N_6O_4S^+$ 493.2592; measured 493.2590.

tert-Butyl (4-((4-Acetamidophenyl)amino)-1,3,5-triazin-2-yl)-L-leucinate (26). To a stirred solution of **24** (50 mg, 0.167 mmol) in THF and water (5 mL, 0.5 mL) were added **18c** (25 mg, 0.15 mmol, 1 equiv) and potassium carbonate (31 mg, 0.22 mmol, 1.35 equiv). This was stirred at room temperature overnight. EtOAc and water (50 mL) were added to the mixture, and the organic layers were separated. The aqueous layer was washed with EtOAc (50 mL × 3), and the organic layers were combined and washed with water (30 mL × 2) and brine (20 mL), dried over anhydrous MgSO$_4$, and concentrated *in vacuo*. The crude product was purified by column chromatography MeOH/DCM (0−10%) to give a beige solid (33 mg, 48% yield).

^{1}H NMR (600 MHz, chloroform-*d*) δ 8.23 (d, *J* = 31.1 Hz, 1H), 7.58−7.44 (m, 3H), 7.20 (s, 1H), 5.78 (s, 1H), 4.64 (q, *J* = 3.4 Hz, 0H), 4.54 (td, *J* = 8.5, 5.8 Hz, 1H), 2.18 (d, *J* = 2.8 Hz, 3H), 1.52−1.49 (m, 2H), 1.44 (s, 6H), 1.26 (s, 1H), 1.02−0.93 (m, 9H). ^{13}C NMR (151 MHz, chloroform-*d*) δ 172.23, 169.61, 168.21, 165.08, 121.42, 120.59, 82.01, 53.04 (d, *J* = 17.9 Hz), 41.73 (d, *J* = 48.5 Hz), 28.12, 25.04 (d, *J* = 13.1 Hz), 24.65, 22.97, 22.86, 22.35.

^{13}C NMR (151 MHz, chloroform-*d*) δ 172.23, 169.61, 168.21, 165.08, 121.42, 120.59, 82.01, 53.04 (d, *J* = 17.9 Hz), 41.73 (d, *J* = 48.5 Hz), 28.12, 25.04 (d, *J* = 13.1 Hz), 24.65, 22.97, 22.86, 22.35.

HRESIMS [M + H] calcd for $C_{21}H_{31}N_6O_3^+$ 452.2452; measured 452.2456.

(4-((4-Acetamidophenyl)amino)-1,3,5-triazin-2-yl)-L-leucine (27). To a suspension of **26** (130 mg, 0.314 mmol) in CH$_2$Cl$_2$ (1 mL) at r.t. was added trifluoroacetic acid (0.2 mL), and the mixture was stirred at r.t. for 3 h (TLC, LCMS). The solvent was then removed *in vacuo* (in fume hood), and the residue was triturated with c-Hex:Et$_2$O, 1:1. The solid formed was collected by filtration, azeotroped (DCE, 10 mL × 2), and dried to afford the title compound as a white solid (0.08 g, 0.223 mmol, 71%).

^{1}H NMR (600 MHz, DMSO-*d*$_6$) δ/ppm: 9.85 (m, 1H), 8.20 (m, 1H), 7.58 (d, 1H, *J* = 8.3 Hz), 7.51−7.47 (m, 2H), 4.44 (m, 1H), 2.02 (s, 3H), 1.76−1.68 (m, 2H), 0.92 (d, 3H, *J* = 6.3 Hz), 0.88−0.85 (m, 3H).

^{13}C NMR (150 MHz, DMSO-*d*$_6$) δ/ppm: 174.5, 174.1, 168.0, 134.7, 133.9, 120.6, 119.8, 119.2, 51.9, 24.5, 23.9, 23.0, 22.9, 21.3, 21.1.

LCMS [M + H] calcd for: $C_{17}H_{23}N_6O_3^+$ 359.18; measured: 359.20.

Isopropyl (4-((4-Acetamidophenyl)amino)-1,3,5-triazin-2-yl)-L-leucinate (28). A solution of **27** (100 mg, 0.279 mmol), CBr$_4$ (92.5 mg, 0.279 mmol), and anhydrous iPrOH (5 mL) was heated in the microwave at 150 °C for 3 h. After the reaction was complete (analysis by TLC), the excess alcohol was removed *in vacuo*. Further purification was achieved by flash chromatography with ethyl acetate/hexane. Column chromatography (19:1, CH$_2$Cl$_2$:MeOH) afforded the title compound as a white solid (0.043 g, 0.107 mmol, 38%).

^{1}H NMR (600 MHz, DMSO-*d*$_6$) δ/ppm: 9.85 (m, 1H), 8.15 (d, 1H, *J* = 12.9 Hz), 7.59 (d, 1H, *J* = 8.8 Hz), 7.51−7.46 (m, 2H), 4.88 (m, 1H), 4.40 (m, 1H), 3.35 (s, 6H), 2.01 (s, 3H), 1.75−1.68 (m, 2H), 1.52 (m, 1H), 1.18 (d, 1H, *J* = 6.2 Hz), 1.15 (dd, 3H, *J* = 6.1, 3.8 Hz), 0.92 (d, 3H, *J* = 6.3 Hz), 0.86 (t, 3H, *J* = 6.4 Hz).

^{13}C NMR (150 MHz, DMSO-*d*$_6$) δ/ppm: 172.7, 167.9, 165.6, 164.9, 134.6, 134.2, 119.2, 119.0, 68.0, 67.8, 52.1, 24.5, 24.4, 24.0, 22.9, 22.8, 21.6, 21.5, 21.3, 21.2.

LCMS [M + H] calcd for $C_{20}H_{29}N_6O_3$: 401.2; measured: 401.2.

Cyclopentyl (4-((4-Acetamidophenyl)amino)-1,3,5-triazin-2-yl)-L-leucinate (29). A solution of the **27** (100 mg, 0.279 mmol), CBr$_4$ (92.5 mg, 0.279 mmol), and anhydrous c-Pentanol (2 mL) was irradiated in the MW at 150 °C for 1 h. After the reaction was complete (analysis by TLC), the excess alcohol was removed *in vacuo*.

Column chromatography (19:1, CH$_2$Cl$_2$:MeOH) afforded the title compound as a white solid (0.014 g, 0.033 mmol, 24%).

^{1}H NMR (600 MHz, DMSO-*d*$_6$) δ/ppm: 9.85 (d, 1H, *J* = 10.0 Hz), 8.15 (d, 1H, *J* = 13.9 Hz), 7.57 (d, 1H, *J* = 8.9 Hz), 7.50−7.45 (m, 2H), 5.06 (m, 1H), 5.03 (m, 1H), 4.42−4.34 (m, 2H), 2.01 (s, 3H), 1.75−1.68 (m, 3H), 1.57−1.43 (m, 5H), 0.92 (d, 3H, *J* = 6.3 Hz), 0.86 (dd, 3H, *J* = 6.3, 3.7 Hz).

^{13}C NMR (150 MHz, DMSO-*d*$_6$) δ/ppm: 172.7, 165.1, 134.2, 120.6, 77.1, 52.5, 41.8, 41.5, 32.8, 32.6, 29.8, 25.04, 24.95, 24.7, 23.8, 23.7, 22.96, 22.87, 22.3, 22.1.

LCMS [M − H] calcd for $C_{22}H_{29}N_6O_3^-$ 425.24; measured 425.80.

(S)-2-((4-((4-Acetamidophenyl)amino)-1,3,5-triazin-2-yl)amino)-N-methoxy-N,4-dimethylpentanamide (32). To a solution of **30** (167 mg, 0.632 mmol) and Weinreb amide L-leucine HCl (200 mg, 0.949 mmol) in dry DMF (2 mL) at r.t. was added triethylamine (0.22 mL, 1.58 mmol) and the mixture was stirred at 80 °C for 3 h (TLC, LCMS). To the reaction was then added water, and the resultant solid was filtered, washed with water, and then dried. Column chromatography (19:1, CH$_2$Cl$_2$:MeOH) afforded the title compound as a white solid (0.038 g, 0.094 mmol, 15%).

^{1}H NMR (600 MHz, CDCl$_3$) δ/ppm: 8.22 (m, 1H), 7.51 (d, 2H, *J* = 8.8 Hz), 7.47−7.41 (m, 2H), 5.28 (m, 1H), 3.91 (s, 1H), 3.61 (s, 1H), 3.22 (m, 3H), 2.18 (d, 3H, *J* = 5.9 Hz), 1.76 (m, 1H), 1.66−1.56 (m, 4H), 1.00−0.90 (m, 5H).

LCMS [M + H] calcd for $C_{19}H_{28}N_7O_3^+$ 402.22; measured: 402.10.

(S)-N-(4-((4-((1-Hydroxy-4-methylpentan-2-yl)amino)-1,3,5-triazin-2-yl)amino)phenyl)acetamide (33). To a solution of **30** (100 mg, 0.379 mmol) and L-leucinol (63.5 mg, 0.541 mmol) in dry DMF (2 mL) at r.t. was added triethylamine (0.056 mL, 0.397 mmol), and the mixture was stirred at 80 °C for 3 h (TLC, LCMS). To the reaction was then added water, and the resultant solid was filtered, washed with water, and then dried. Column chromatography (4:1, EtOAc:c-Hex → EtOAc → 9:1, EtOAc:MeOH) afforded the title compound as a white solid (0.029 g, 0.084 mmol, 23%).

^{1}H NMR (600 MHz, DMSO) δ/ppm: 9.83 (s, 1H), 9.43 (m, 1H), 7.68 (s, 1H), 7.63 (d, 1H, *J* = 7.7 Hz), 7.45 (dd, 2H, *J* = 8.9, 4.0 Hz), 4.71−4.67 (m, 2H), 2.01 (s, 3H), 1.63 (m, 1H), 1.38 (m, 2H), 0.89 (dd, 3H, *J* = 6.5, 3.4 Hz), 0.87=0.84 (m, 3H).

^{13}C NMR (150 MHz, DMSO) δ/ppm: 167.9, 165.4, 164.9, 134.9, 134.0, 119.1, 63.9, 63.5, 59.8, 55.0, 50.1, 29.0, 24.4, 23.9, 23.5, 22.2, 21.9.

LCMS [M + H] calcd for $C_{17}H_{25}N_6O_2^+$ 345.20; measured: 345.30.

tert-Butyl (4-((4-Acetamidophenyl)amino)-1,3,5-triazin-2-yl)-D-leucinate (34). To a solution of **30** (100 mg, 0.379 mmol) and *t*-Bu D-leucine HCl (121 mg, 0.54 mmol) in dry DMF (2 mL) at r.t. was added triethylamine (0.126 mL, 0.9 mmol), and the mixture was stirred at 80 °C for 3 h (TLC, LCMS). To the reaction was then added water, and the resultant solid was filtered, washed with water, and then dried. Column chromatography (7:3, EtOAc:cHex) followed by reversed-phase column chromatography (11:9, MeCN:H$_2$O) afforded the title compound as a white solid (0.079 g, 0.191 mmol, 50%).

^{1}H NMR (600 MHz, DMSO-*d*$_6$) δ/ppm: 9.82 (s, 1H), 9.52 (m, 1H), 8.14 (m, 1H), 7.87 (s, 1H), 7.69 (s, 1H), 7.61 (d, 1H, *J* = 8.6 Hz), 7.52−7.46 (m, 2H), 4.33 (m, 1H), 2.01 (s, 3H), 1.76−1.65 (m, 2H), 1.52 (m, 1H), 1.39 (s, 3H), 1.35 (s, 6H), 0.92 (m, 3H), 0.86 (m, 3H).

^{13}C NMR (150 MHz, DMSO-*d*$_6$) δ/ppm: 172.4, 172.3, 167.9, 165.6, 165.0, 134.6, 134.2, 119.3, 119.0, 80.4, 52.6, 27.7, 27.6, 24.6, 24.4, 23.9, 22.9, 22.8, 21.34, 21.28.

LCMS [M + H] calcd for $C_{21}H_{31}N_6O_3^+$ 415.24; measured: 415.30.

tert-Butyl (4-((4-Acetamidophenyl)amino)-1,3,5-triazin-2-yl)-L-valinate (35). To a solution of **30** (100 mg, 0.379 mmol) and *t*-Bu valine HCl (113 mg, 0.54 mmol) in dry DMF (2 mL) was added triethylamine (0.126 mL, 0.9 mmol) at r.t., and the mixture was stirred at 80 °C for 3 h (TLC, LCMS). The reaction was cooled, water was added, and the resultant solid was filtered, washed with water and then diethyl ether, and dried. Reversed-phase column chromatography (2:3, MeCN:H$_2$O) afford the title compound as a white solid (0.040 g, 0.100 mmol, 26%).

^{1}H NMR (600 MHz, CDCl$_3$) δ/ppm: 8.22 (m, 1H), 7.56−7.40 (m, 4H), 6.01 (s, 1H), 4.46 (m, 1H), 2.25 (m, 1H), 2.18 (s, 3H), 1.48 (s, 3H), 1.46 (s, 6H), 1.04−0.97 (m, 6H).

^{13}C NMR (150 MHz, CDCl$_3$) δ/ppm: 171.0, 168.3, 166.1, 165.6, 165.3, 134.3, 133.7, 120.6, 82.2, 59.4, 59.1, 31.6, 31.3, 28.2, 24.6, 18.3, 18.1.

LCMS [M + H] calcd for C$_{20}$H$_{29}$N$_6$O$_3^+$ 401.22; measured 401.30.

tert-Butyl (4-((4-Acetamidophenyl)amino)-1,3,5-triazin-2-yl)-glycinate (**36**). To a solution of **30** (100 mg, 0.379 mmol) and *t*-Bu glycine HCl (95 mg, 0.569 mmol) in dry DMF (2 mL) at r.t. was added triethylamine (0.133 mL, 0.95 mmol), and the mixture was stirred at 80 °C for 3 h (TLC, LCMS). To the reaction was then added water, and the resultant solid was filtered, washed with water, and then dried. Column chromatography (1:4, c-Hex, EtOAc) afforded the title compound as a white solid (0.036 g, 0.173 mmol, 46%).

^{1}H NMR (600 MHz, DMSO-d_6) δ/ppm: 9.82 (s, 1H), 9.54 (d, br, J = 48.0 Hz, 1H), 8.16 (d, J = 30.0 Hz, 1H), 7.54−7.94 (m, 3H), 7.44−7.52 (m, 2H), 3.85−3.93 (m, 2H), 2.02 (s, 3H), 1.41 (s, 3H), 1.37 (s, 6H).

^{13}C NMR (150 MHz, DMSO-d_6) δ/ppm: 169.3 (d, J = 19.5 Hz), 167.8, 165.6 (d, J = 19.5 Hz), 165.2, 165.1, 134.6, 134.2, 120.2 (d, J = 54.0 Hz), 119.0 (d, J = 54.0 Hz), 80.6 (d, J = 7.5 Hz), 42.7, 27.7 (d, J = 10.5 Hz), 23.8 (d, J = 4.5 Hz).

LCMS [M + H] calcd for: C$_{17}$H$_{23}$N$_6$O$_3^+$ 359.18; measured: 359.20.

tert-Butyl (S)-2-((4-((4-Acetamidophenyl)amino)-1,3,5-triazin-2-yl)amino)-3,3-dimethylbutanoate (**37**). To a solution of **30** (100 mg, 0.379 mmol) and H-Tle-OtBu HCl (127 mg, 0.569 mmol) in dry DMF (2 mL) at r.t. was added triethylamine (0.133 mL, 0.948 mmol), and the mixture was stirred at 80 °C for 3 h (TLC, LCMS). To the reaction was then added water, and the resultant solid was filtered, washed with water, and then dried. Column chromatography (9:1, CH$_2$Cl$_2$:MeOH) followed by reversed-phase column chromatography (1:1, MeCN:H$_2$O) afforded the title compound as a white solid (0.011 g, 0.027 mmol, 7%).

^{1}H NMR (600 MHz, DMSO-d_6) δ/ppm: 9.86 (s, 1H), 9.57 (m, 1H), 8.16 (m, 1H), 7.63 (d, 2H, J = 7.0 Hz), 7.50 (d, 2H, J = 8.8 Hz), 4.16 (s, 1H), 2.01 (m, 3H), 1.41 (s, 3H), 1.35 (s, 6H), 1.04 (s, 6H), 1.03 (s, 3H).

LCMS [M + H] calcd for C$_{21}$H$_{31}$N$_6$O$_3^+$ 415.24; measured: 414.90.

tert-Butyl 2-((4-((4-Acetamidophenyl)amino)-1,3,5-triazin-2-yl)-amino)-2-methylpropanoate (**38**). To a solution of **30** (75 mg, 0.284 mmol) and HAib-OtBu (48 mg, 0.301 mmol) in dry DMF (2 mL) at r.t. was added potassium carbonate (43 mg, 0.312 mmol), and the mixture was stirred at 80 °C for 3 h. The reaction was then cooled and partitioned between EtOAc and water, and the organic layer was washed with sat. aq. LiCl. The organic layer was then dried and evaporated. Column chromatography (19:1, CH$_2$Cl$_2$:MeOH) followed by reversed-phase column chromatography (3:7, MeCN:H$_2$O) afforded the title compound as a white solid (0.011 g, 0.029 mmol, 10%).

^{1}H NMR (600 MHz, DMSO-d_6) δ/ppm: 9.81 (m, 1H), 8.12 (m, 1H), 7.56 (d, 2H, J = 8.9 Hz), 7.47 (t, 2H, J = 8.3 Hz), 2.01 (s, 3H), 1.48 (s, 4H), 1.43 (s, 2H), 1.33 (s, 6H).

LCMS [M + H] calcd for C$_{19}$H$_{27}$N$_6$O$_3^+$ 387.21; measured: 387.20.

tert-Butyl (4-((4-Acetamidophenyl)amino)-1,3,5-triazin-2-yl)-L-alaninate (**39**). To a solution of **30** (100 mg, 0.379 mmol) and *t*-Bu alanine HCl (103 mg, 0.568 mmol) in dry DMF (2 mL) at r.t. was added dry triethylamine (0.133 mL, 0.948 mmol), and the mixture was stirred at 80 °C for 3 h (TLC, LCMS). The reaction was cooled, water was added, and the resultant solid was filtered, washed with water, and then dried. Column chromatography (8:2, EtOAc:cHex) followed by reversed-phase column chromatography (1:1, MeCN:-H$_2$O) afforded the *title compound* as a white solid (0.035 g, 0.094 mmol, 25%).

^{1}H NMR (600 MHz, DMSO-d_6) δ/ppm: 9.82 (s, 1H), 9.52 (m, 1H), 9.15 (m, 1H), 7.59 (d, 2H, J = 9.0 Hz), 7.52−7.47 (m, 2H), 4.31 (m, 1H), 2.02 (s, 3H), 1.39 (s, 3H), 1.38−1.30 (m, 9H).

^{13}C NMR (150 MHz, DMSO-d_6) δ/ppm: 172.4, 167.9, 165.5, 164.7, 134.6, 134.2, 119.3, 119.0, 80.4, 49.8, 27.7, 24.0, 17.0.

LCMS [M + H] calcd for C$_{18}$H$_{25}$N$_6$O$_3^+$ 373.19; measured 373.20.

tert-Butyl (S)-2-((4-((4-Acetamidophenyl)amino)-1,3,5-triazin-2-yl)amino)-2-cyclohexylacetate (**40**). To a solution of **30** (100 mg, 0.379 mmol) and H-L-cyclohexyl-Gly-OtBu·HCl (142 mg, 0.569 mmol) in dry DMF (2 mL) at r.t. was added triethylamine (0.133 mL, 0.948 mmol), and the mixture was stirred at 80 °C for 3 h (TLC, LCMS). To the reaction was then added water, and the resultant solid was filtered, washed with water, and then dried. Column chromatography (9:1, CH$_2$Cl$_2$:MeOH) followed by reversed-phase column chromatography (11:9, MeCN:H$_2$O) afforded the title compound as a white solid (0.046 g, 0.104 mmol, 28%).

^{1}H NMR (600 MHz, DMSO-d_6) δ/ppm: 9.86 (s, 1H), 9.56 (s, 1H), 8.14 (m,1H), 7.76 (m, 1H), 7.61 (d, 2H, J = 8.1 Hz), 7.53−7.48 (m, 2H), 4.24 (t, 1H, J = 7.4 Hz), 2.02 (s, 3H), 1.85−1.56 (m, 6H), 1.40 (s, 3H), 1.34 (s, 6H), 1.26−1.07 (m, 5H).

^{13}C NMR (150 MHz, DMSO-d_6) δ/ppm: 171.2, 167.9, 165.5, 165.1, 165.0, 134.6, 134.2, 120.0, 119.0, 80.5, 59.2, 29.0, 28.8, 28.7, 27.7, 25.6, 24.0.

LCMS [M + H] calcd for C$_{23}$H$_{33}$N$_6$O$_3^+$ 441.25; measured 440.90.

tert-Butyl (4-((4-Acetamidophenyl)amino)-1,3,5-triazin-2-yl)-L-phenylalaninate (**41**). To a solution of **30** (100 mg, 0.379 mmol) and *t*-OBu phenylalanine HCl (140 mg, 0.542 mmol) in dry DMF (2 mL) at r.t. was added triethylamine (0.127 mL, 0.902 mmol), and the mixture was stirred at 80 °C for 3 h (TLC, LCMS). To the reaction was then added water, and the resultant solid was filtered, washed with water, and then dried. Reversed-phase column chromatography (9:11, MeCN:H$_2$O) afford the title compound as a white solid (0.073 g, 0.163 mmol, 43%).

^{1}H NMR (600 MHz, DMSO-d_6) δ/ppm: 9.87 (s, 1H), 9.56 (m, 1H), 8.16 (m, 1H), 7.61 (d, 2H, J = 8.7 Hz), 7.54 (d, 1H, J = 8.8 Hz), 7.52 (d, 1H, J = 8.8 Hz), 7.34−7.31 (m, 4H), 7.25 (m, 1H), 4.54 (s, 1H), 3.12−3.08 (m, 2H), 2.06 (s, 3H), 1.37 (s, 3H), 1.34 (s, 6H).

^{13}C NMR (150 MHz, DMSO-d_6) δ/ppm: 171.3, 167.9, 165.6, 164.9, 164.8, 158.4, 137.8, 134.5, 134.3, 129.1, 128.3, 126.5, 119.3, 119.0, 80.7, 80.6, 55.8, 27.6, 27.5, 23.9.

LCMS [M + H] calcd for C$_{24}$H$_{29}$N$_6$O$_3^+$ 449.22; measured 449.30.

tert-Butyl (4-((4-Acetamidophenyl)amino)-1,3,5-triazin-2-yl)-L-tyrosinate (**42**). To a solution of **30** (75 mg, 0.284 mmol) and *t*-OBu tyrosine (71 mg, 0.298 mmol) in dry DMF (2 mL) at room temperature was added potassium carbonate (43 mg, 0.312 mmol), and the mixture was stirred at 80 °C for 3 h. The reaction was cooled and partitioned between ethyl acetate and saturated citric acid. The organic layer was washed with saturated aqueous lithium chloride, dried, and evaporated. Column chromatography (30:1, CH$_2$Cl$_2$:MeOH) followed by reversed-phase column chromatography (2:3, MeCN:H$_2$O) afforded the title compound as a white solid (0.020 g, 0.043 mmol, 15%).

^{1}H NMR (600 MHz, DMSO-d_6) δ/ppm: 9.86 (m, 1H), 9.23 (m, 1H), 8.12 (m, 1H), 7.58 (d, 2H, J = 8.5 Hz), 7.53−7.46 (m, 2H), 7.10−7.02 (m, 2H), 6.66 (m, 2H), 4.39 (m, 1H), 3.00−2.87 (m, 2H), 2.02 (s, 3H), 1.33 (s, 3H), 1.30 (s, 6H).

^{13}C NMR (150 MHz, DMSO-d_6) δ/ppm: 174.5, 172.8, 170.0, 153.9, 134.3, 133.4, 141.7, 130.3, 129.6, 119.1, 114.8, 114.1, 80.0, 67.5, 59.8, 56.2, 42.7, 33.1, 27.9, 27.7, 27.5, 23.9, 21.2, 14.2.

LCMS [M + H] calcd for C$_{24}$H$_{29}$N$_6$O$_4^+$ 464.22; measured: 465.20.

tert-Butyl (S)-2-((4-((4-Acetamidophenyl)amino)-1,3,5-triazin-2-yl)amino)-3-(4-fluorophenyl)propanoate (**43**). To a solution of **30** (50 mg, 0.190 mmol) and 4-fluorophenylalanine-OtBu HCl (58 mg, 0.209 mmol) in dry DMF (1 mL) at r.t. was added triethylamine (0.059 mL, 0.417 mmol), and the mixture was stirred at 80 °C for 3 h (TLC, LCMS). To the reaction was then added water, and the resultant solid was filtered, washed with water, and then dried. Reversed-phase column chromatography (3:2, MeCN:H$_2$O) afforded the title compound as a white solid (0.014 g, 0.030 mmol, 16%).

^{1}H NMR (600 MHz, DMSO-d_6) δ/ppm: 9.84 (s, 1H), 8.11 (m, 1H), 7.57 (d, 1H, J = 8.8 Hz), 7.52−7.46 (m, 2H), 7.36−7.30 (m, 2H), 7.11 (t, 2H, J = 8.7 Hz), 4.46 (m, 1H), 3.09−3.00 (m, 2H), 2.02 (s, 3H), 1.33 (s, 3H), 1.30 (s, 6H).

^{13}C NMR (150 MHz, DMSO-d_6) δ/ppm: 171.1, 167.9, 165.6, 164.92, 164.85, 160.3, 134.5, 134.3, 134.0, 131.03, 130.98, 119.3, 119.0, 115.0, 114.9, 80.8, 80.7, 27.6, 27.5, 23.9.

LCMS theoretical [$C_{24}H_{27}FN_6O_3$ + H] 467.21; measured: 468.30.

tert-Butyl (S)-3-((4-((4-Acetamidophenyl)amino)-1,3,5-triazin-2-yl)amino)-4-phenylbutanoate (**44**). To a solution of **30** (100 mg, 0.379 mmol) and *tert*-butyl (3S)-3-amino-4-phenylbutanoate (98 mg, 0.413 mmol) in dry DMF (2 mL) at r.t. was added triethylamine (0.06 mL), and the mixture was stirred at 80 °C for 3 h (TLC, LCMS). To the reaction was then added water, and the resultant solid was filtered, washed with water, and then dried. Reversed-phase column chromatography (2:3, MeCN:H$_2$O) afforded the title compound as a white solid (76 mg, 0.164 mmol, 43%).

^{1}H NMR (600 MHz, DMSO-d_6) δ/ppm: 9.86 (m, 1H), 8.08 (m, 1H), 7.71−7.44 (m, 5H), 7.30−7.25 (m, 2H), 7.24−7.16 (m, 3H), 4.59 (m, 1H), 2.82 (m, 1H), 2.72 (m, 1H), 2.02 (m, 3H), 1.31 (m, 9H).

^{13}C NMR (150 MHz, DMSO-d_6) δ/ppm: 170.1, 167.9, 165.5, 164.5, 134.7, 134.2, 129.2, 128.31, 128.27, 126.3, 126.2, 120.3, 119.3, 119.0, 79.9, 49.0, 27.7, 27.6, 24.0, 23.9.

LCMS [M + H] calcd for $C_{25}H_{31}N_6O_3^+$ 463.24; measured 463.30.

tert-Butyl (S)-3-((4-((4-Acetamidophenyl)amino)-1,3,5-triazin-2-yl)amino)-5-phenylpentanoate (**45**). To a solution of **30** (96 mg, 0.364 mmol) and *tert*-butyl homophenylalanine (100 mg, 0.401 mmol) in dry DMF (2 mL) at r.t. was added triethylamine (0.061 mL), and the mixture was stirred at 80 °C for 3 h (TLC, LCMS). To the reaction was then added water, and the resultant solid was filtered, washed with water, and then dried. Column chromatography (19:1, CH$_2$Cl$_2$:MeOH) followed by reversed-phase column chromatography (1:1, MeCN:H$_2$O) afforded the title compound as a white solid (0.041 g, 0.089 mmol, 24%).

^{1}H NMR (600 MHz, DMSO-d_6) δ/ppm: 9.85 (m, 1H), 8.15 (s, 1H), 7.57 (m, 2H), 7.50 (m, 2H), 7.31−7.16 (m, 5H), 4.24 (m, 1H), 2.75 (m, 1H), 2.68 (m, 1H), 2.02 (s, 3H), 1.39 (s, 3H), 1.33 (s, 6H).

^{13}C NMR (150 MHz, DMSO-d_6) δ/ppm: 172.0, 167.9, 165.5, 165.1, 141.1, 134.6, 134.2, 128.5, 128.4, 126.0, 119.3, 119.0, 80.6, 32.8, 31.9, 31.7, 27.8, 27.7, 27.6, 24.0, 23.8.

LCMS [M − H] calcd for $C_{26}H_{31}N_6O_3^-$ 463.24; measured: 463.30.

*(S)-N-(4-((4-((1-(tert-Butoxy)-4-methylpentan-2-yl)amino)-1,3,5-triazin-2-yl)amino)phenyl)acetamide (**46**).* To a solution of **33** (20 mg, 0.058 mmol) and molecular sieves and MTBE (0.5 mL) was added dropwise conc. sulfuric acid (10 μL, 0.174 mmol), and the reaction was stirred at r.t. for 5 h. Once the starting material had fully dissolved, the reaction was then slowly quenched with saturated aqueous solution of sodium bicarbonate. The organic layer was separated, and the aqueous layer was extracted twice with ethyl acetate. The combined organic layers were washed with water, dried over magnesium sulfate, and the solvent was removed *in vacuo*. Column chromatography (19:1, CH$_2$Cl$_2$:MeOH) afforded the title compound as a white solid (0.004 g, 0.0099 mmol, 17%).

^{1}H NMR (600 MHz, DMSO-d_6) δ/ppm: 9.83 (s, 1H), 9.45 (m, 1H), 7.70−7.61 (m, 2H), 7.46 (dd, 2H, J = 8.9, 2.0 Hz), 7.30 (s, 1H), 4.10 (s, 1H), 3.18 (m, 1H), 2.01 (s, 3H), 1.63 (m, 1H), 1.43−1.39 (m, 2H), 1.11 (s, 9H), 0.88 (d, J = 6.7 Hz), 0.85−0.81 (m, 3H).

LCMS [M + H] calcd for $C_{21}H_{33}N_6O_2^+$ 401.26; measured: 401.30.

*(4-((4-Acetamidophenyl)amino)-1,3,5-triazin-2-yl)-L-phenylalanine (**47**).* To a suspension of **41** (20 mg, 0.045 mmol) in DCM (2 mL) at room temperature was added trifluoroacetic acid (0.4 mL), and the mixture was stirred at room temperature for 18 h. The solvent was then removed *in vacuo*, and the residue was triturated with *i*Pr$_2$O. The solid formed was collected by filtration, azeotroped with dichloromethane, and dried to afford the title compound (15 mg, 0.041 mmol, 91%).

^{1}H NMR (600 MHz, DMSO-d_6) δ/ppm: 9.85 (m, 1H), 8.14 (s, 1H), 7.53 (d, 2H, J = 8.4 Hz), 7.48 (dd, 2H, J = 9.5, 2.7 Hz), 7.31−7.25 (m, 4H), 7.19 (m, 1H), 4.58 (m, 1H), 3.16 (m, 1H), 3.03 (m, 1H), 2.01 (m, 3H).

LCMS [M + H] calcd for $C_{20}H_{21}N_6O_3^+$ 393.16; measured: 393.20.

SPR Assay. All SPR analysis was performed on a BIAcore T200 system using Series S CM5 sensor chips. All sensorgrams were double-referenced by subtracting the response on a reference flow cell and a blank sample. Ligands were evaluated against the FL (27−541) NPR-C Protein. Human FL NPR-C (27−541)-10His-Flag was covalently attached to a CM5 chip via amine coupling[14] with a surface density of 5000 RU. Binding of agonists (150−0 μM) was analyzed by multicycle sequential injections at a flow rate of 30 μL/min (60 s association time) followed by undisturbed dissociation (30 s) during which curves returned to baseline. Peptide antagonist M372049 was used as a positive control. Agonists were dissolved in dimethyl sulfoxide (DMSO), and the final sample solutions for kinetic affinity assays were 1% DMSO in 1× phosphate-buffered saline P20 buffer (PBS-P, Cat no 28995084, GE Healthcare Ltd.). DMSO solvent effects were corrected for with eight calibration solutions (0.5−1.8% DMSO in PBS-P). Equilibrium constants (K_D) were calculated using the affinity model, assuming simple 1:1 (Langmuir) binding. Data processing and analysis were performed using BIAevaluation and OriginPro software. The theoretical R_{max} (the maximal feasible signal in a ligand−analyte pair) for each compound/protein pair was calculated using eq 1[35]

$$R_{max} = R_{ligand} \cdot \left(\frac{Mr_{analyte}}{Mr_{ligand}} \right) \cdot V_{ligand}$$

(1)

where R_{ligand} is the amount of protein loaded in the SPR chip in response units; $Mr_{analyte}$ is the molecular weight of the compound of interest; Mr_{ligand} is the molecular weight of the immobilized protein; and V_{ligand} is the stoichiometry of the binding interaction between the ligand and the analyte. The experimentally observed R_{max} was then calculated as a percentage of the theoretical R_{max} as a quality control measure. An experimental R_{max} < 100% of the theoretical R_{max} was considered sensible and indicative of genuine binding.[35]

FP Assay. All experiments were performed using PBS-P buffer, a 100 μL final volume, and 1% DMSO. Protein titration experiments were performed at 1.5, 15, 150, and 1500 pM P19 probe concentration. To achieve a balance of protein consumption and fluorescence polarization dynamic readout range for competition experiments, the concentrations selected were 20 nM protein concentration and 150 pM P19 probe concentration. Keeping the appropriate reaction plate or tubes on ice, the optimized fluorescence polarization samples were prepared in the flowing order—ligand in PBS-P-4% DMSO (2400−1.097 μM, 25 μL), NPR-C protein in PBS-P buffer (128 nM, 25 μL), and P19 probe in PBS-P buffer (300 pM, 50 μL). Fluorescence polarization competition experiments against the Flu-P19 probe were performed with varying concentrations of ligand (600−0.274 μM) and their fluorescence polarization readout measured and normalized to experimental controls (buffer + probe, protein + probe) using a BMG Labtech Omega Pherastar plate reader (filter settings: 485 nm [excitation] and 520 nm [emission]). Background fluorescence polarization was blanked using a PBS-P-1% DMSO buffer only control. Raw data were processed using OriginPro curve fitting software to obtain the EC$_{50}$s.

Organ Bath. The vascular reactivity of rat thoracic aortic and murine mesenteric arterial (from wild-type and NPR-C$^{-/-}$ animals) vascular ring preparations was determined using classical tissue bath pharmacology, as we have described previously.[36] To confirm the specific NPR-C response on rat small mesenteric artery, some vessels were incubated with M372049 (10 μM) or osteocrin (100 nM) for 15 min prior to testing the vasorelaxant properties of the compounds. All studies conformed to the U.K. Animals (Scientific Procedures) Act of 1986 and had approval from a local Animal Welfare and Ethical Review Body. NPR-C$^{-/-}$ mice were the kind gift of Prof O. Smithies (University of North Carolina at Chapel Hill, Chapel Hill, NC) and Wistar rats were purchased from Charles River U.K. Animals were grouped and housed in individually ventilated cages with free access to chow and water in a 12 h light/dark cycle (7 a.m. to 7 p.m.) and controlled temperature and humidity (21 °C and 45% relative humidity). Only male animals were used in this study.

HeLa Assay. HeLa cells were selected to test NPR-C activation *in vitro* due to their higher expression of NPR-C over NPR-A or NPR-B.[37] The cells were maintained in Dulbecco's modified Eagle's

medium (DMEM) high-glucose media supplemented with 10% heat-inactivated bovine serum, 100 U/mL penicillin, and 100 U/mL streptomycin in a humidified incubator at 5% (v/v) CO_2.

NPR-C contains a G_i binding domain that upon activation of the receptor reduces cAMP synthesis by inhibiting adenylyl cyclase activity.[6] The ability of NPR-C agonists to inhibit forskolin-induced cAMP production was tested in 80% confluent HeLa cells.

On the assay day, media was changed and the cells were left to stabilize for 4 h. Cultures were preincubated with the NPR-C selective agonist cANF$^{4-23}$ (100 nM), **1**, **17**, **26**, and **41** (100 μM), for 10 min prior to the addition of forskolin (10 μM). 3-Isobutyl-1-methylxanthine (IBMX, 1 mM) was added alongside the agonists to prevent cAMP degradation. In some experiments, to test the specificity of the agonism, the cells were treated with the NPR-C antagonists osteocrin (100 nM) or M372049 (10 μM) for 10 min prior to the addition of the agonists. After 20 min of forskolin activation, the cells were lysed in 1% Triton-X/0.1 M HCl buffer, spun at 18 620 g for 2 min at 4 °C, and supernatants were frozen for further analyses.

The activation of NPR-A and NPR-B induces the production of the secondary messenger cGMP. NPR-A and NPR-B agonisms were tested by measuring cGMP formation in HeLa cells. The cells were grown and maintained as described above. After 4 h equilibration, the ability of ANP (1 μM), CNP (1 μM), cANF$^{4-23}$ (1 μM), and compounds **1**, **17**, **26**, **27**, **39**, **40**, **41**, **43**, **44**, and **45** (10 μM) was tested in the presence of IBMX (1 mM). After 30 min, the reaction was stopped as described above and the lysates were snap-frozen for further analyses.

The supernatants obtained as described above were used for cAMP and cGMP measurements using an ELISA kit as instructed by the manufacturer (Enzo Life Sciences, Farmingdale) and normalized to the protein concentration of the sample measured by BCA protein assay (Thermo Scientific, MA).

ADME and PK Data. Determination of ADME and PK parameters (clearance and half-life in rat hepatocyte and human plasma, plasma protein binding, cyp P450 inhibition, and *in vivo* studies) was conducted by WuXi AppTech.

Plasma Protein Binding. Binding of compounds and warfarin (positive control) to human and Sprague-Dawley rat plasma protein was determined using equilibrium dialysis, and the concentration of the analyte was determined using the peak area ratio of analyte and internal standard. The results were calculated using the following equations

$$\% \text{ unbound} = 100 * F_C/T_C, \% \text{ bound} = 100 * (1 - F_C/T_C)$$

$$\% \text{ recovery} = 100 * (F_C + T_C)/T_0$$

where T_C is the total compound concentration as determined by the calculated concentration on the retentate side of the membrane; F_C is the free compound concentration as determined by the calculated concentration on the dialysate side of the membrane; and T_0 is the total compound concentration as determined before dialysis.

Stability in Rat Hepatocyte. Cryopreserved rat hepatocytes were tested for cell viability with trypan blue and found to be 80% viable (vendor: BioreclamationIVT; Cat. No. M00005; lot. BSI; pooled of 27 male Sprague-Dawley rats).

Test compounds were provided as a 10 mM stock in DMSO, and 30 mM stock solutions of positive control compounds in DMSO were prepared.

1. 1000× stock was prepared by dilution of 10 and 30 mM stock solution to 1 and 3 mM, respectively, with DMSO in a 96-well plate.

2. 50× intermediate solution: 20 μL of 1000× stock solution was pipetted and mixed with 380 μL of 45% MeOH/H_2O to obtain 50 and 150 μM stock solutions.

3. 5× working solution: 50 μL of 50× intermediate stock solution was pipetted and mixed with 450 μL of prewarmed Williams' medium E to obtain 5 and 15 μM test and control compound solutions, respectively.

4. Spiked 10 μL of 5× Working Solution into appropriate wells in 96-well plates corresponding to T0, T15, T30, T60, and T90 in duplicates. All prelabeled plates with compounds were kept warm in an incubator at 37 °C.

5. Preparation of 0.625×10^6/mL cells suspension: cryopreserved cells were thawed, isolated, and suspended in Williams' Medium E and then diluted with prewarmed Williams' Medium E to 0.625×10^6 cells/mL.

6. The reaction was started by aliquoting 40 μL of 0.625×10^6/mL cells suspension into each well in 96-well plates containing 10 μL compounds to obtain a final concentration of 1 μM test compound and 3 μM control compound.

7. For T15, T30, T60, and T90 sample plates were incubated immediately in an incubator at 37 °C with 5% CO_2. T0 samples were added to stop solution before adding the cells.

8. Medium control (MC) sample plates (T0-MC and T90-MC): T0-MC and T90-MC sample plates were incubated under the same condition as above at the T0 and T90 with Williams' Medium E only without cells.

9. At each corresponding time point, the reaction was stopped by quenching with ACN containing internal standards (IS) at a 1:3 ratio.

10. The sample plates were vortexed immediately and placed on a plate shaker at 500 rpm for 10 min and then centrifuged at 3220g for 20 min.

11. The supernatants were transferred to another set of prelabeled 96-deep-well plates, which contain appropriate dilution solution. The plates were sealed and stored at 4 °C until LC-MS-MS analysis.

The remaining percent of test articles after incubation was calculated by the following equation:

% remaining (at appointed time)

= [(peak area ratios of test article versus internal standard at

appointed time)/(peak area ratios of test article versus internal

standard at 0 min)] × 100%

Human Plasma Stability Assay. Stock solutions (10 mM) of the control and test compounds in DMSO were prepared. Pooled human plasma (EDTA-K2, bioreclamationIVT, cat# HMPLEDTA2, batch BRH1274040) was used in this assay with a minimum number of individuals (3 male and 3 female).

1. The pooled frozen plasma was thawed in a water bath at 37 °C prior to experiment, plasma was centrifuged at 4000 rpm, and the clots (if any) were removed. The pH was adjusted to 7.4 ± 0.1 if required.

2. A 1 mM intermediate solution was prepared by diluting a 10 μL stock solution with 90 μL of DMSO, and 1 mM positive control propantheline was prepared by diluting 5 μL of stock with 35 μL of ultrapure water, and a 1 mM intermediate solution of the positive control enalapril was prepared by diluting 5 μL of stock with 45 μL of DMSO.

3. A 100 μM dosing solution was prepared by diluting 20 μL of intermediate solution with 180 μL of 45% MeOH/H_2O. Propantheline and enalapril were prepared by diluting 10 μL of the intermediate solution with 90 μL of 45% MeOH/H_2O.

4. Blank plasma (196 μL) was spiked with 4 μL of dosing solution to achieve 2 μM of the final concentration in duplicate, and the samples were incubated at 37 °C in a water bath.

5. At each time point (0, 10, 30, 60, and 120 min), 800 μL of stop solution (200 ng/mL tolbutamide and 200 ng/mL labeltalol in 50% CAN/MeOH) was added to precipitate protein and mixed thoroughly.

6. The sample plates were centrifuged at 4000 rpm for 10 min. An aliquot of supernatant (100 μL) was transferred from each well and mixed with 200 μL of ultrapure water. The samples

were shaken at 800 rpm for 10 min before submitting to LC-MS/MS analysis.

Data Analysis. The % remaining of test compound after incubation in plasma was calculated using the following equation:

$$\% \text{ remaining} = 100 \times (\text{PAR at appointed incubation time}$$
$$/\text{PAR at } T_0)$$

where PAR is the peak area ratio of analyte vs. internal standard.

CYP P450 Inhibition. Working solutions (100×) of the test compounds in 1:1 DMSO:MeOH were prepared by dilution of stock solutions in DMSO to provide working concentration ranges of 5, 1.5, 0.5, 0.15, 0.05, 0.015, and 0.005 mM.

Working solutions (100×) of the positive controls (α-naphtho-flavone, ticlopidine, montelukast, sulfaphenazole, (+)-*N*-3-benzylnir-vanol, quinidine, and ketoconazole) were prepared in MeOH at a 300 μM concentration.

NADPH solution (10×) was prepared at a concentration of 10 mM with a 33 mM $MgCl_2$ solution.

Human liver microsome (HLM) working solution (1.27×) was prepared at a concentration of 0.127 mg/mL with PB.

Working solutions (10×) of CYP substrates were prepared with dilution from stocks with PB:

CYP	substrate	concentration (μM)
1A2	Phenacetin	750
2B6	Bupropion	800
2C8	Amodiaquine	20
2C9	Diclofenac	100
2C19	*S*-mephenytoin	200
2D6	Dextromethorphan	100
3A4	Midazolam	20
3A4	testosterone	400

1. Prepare test compound and standard inhibitor working solutions
2. Thaw microsomes on ice
3. Add 20 μL of the substrate solutions to corresponding wells, and add 20 μL of PB
4. Add 2 μL of the test compounds and positive control working solutions to the corresponding wells, and add 2 μL of solvent to no inhibitor and blank wells
5. Prepare HLM working solution
6. Add 158 μL of the HLM working solution to all wells of the incubation plate
7. Prewarm the plate for 10 min in a 37 °C water bath
8. Prepare NADPH cofactor solution
9. Add 20 μL of NADPH cofactor to all incubation wells
10. Mix and incubate for 20 min for CYP2C19 and CYP2D6; 3 min for 3A4 (midazolam); and 10 min for others in a 37 °C water bath
11. At the appropriate time point, terminate the reaction by adding 400 μL of cold stop solution (200 ng/mL tolbutamide and labetalol in acetonitrile)
12. The samples are centrifuged at 4000 rpm for 20 min to precipitate protein
13. Transfer 200 μL of supernatant to 100 μL of HPLC water and shake for 10 min
14. Samples are ready for LC/MS/MS analysis

Data Analysis. SigmaPlot (V.11) was used to plot % control activity versus the test compound concentrations, as well as for nonlinear regression analysis of the data. IC_{50} values were plotted using the equation:

$$y = \frac{\text{max}}{1 + \left(\frac{x}{IC_{50}}\right)^{-\text{hillslope}}}$$

IC_{50} values will be reported as >50 μM when the % inhibition at the highest concentration is less than 50%.

Parallel Artificial Membrane Permeability Assay (PAMPA) Protocol. Test compounds were loaded to the donor plate of the PAMPA sandwich system (Corning Gentest Pre-coated PAMPA Plate System) using dimethyl sulfoxide (DMSO) and phosphate-buffered saline (PBS) (pH 7.4) (5% DMSO, 100 μM, n = 4), and the resultant wells were thoroughly mixed. Two blanks (5% DMSO only) were included for each test compound. Prior to the start of the experiment, an aliquot of each well was then transferred to a UV analysis plate containing acetonitrile (MeCN) for UV analysis of donor plate concentration at t = 0. PBS was then added to the acceptor plate, the acceptor plate was carefully lowered onto the donor plate, and the PAMPA plate assembly was incubated at room temperature for 5 h. At the end of incubation, aliquots from each well of the donor plates were transferred to a 96-well UV−vis analysis plate containing MeCN and each well was thoroughly mixed for UV analysis. Sample aliquots were also taken from the acceptor plate for LCMS analysis using single ion monitoring (SIM) for the m/z^+ and m/z^- for each compound. The results obtained were then quantified against a standard curve for each test sample using either UV−vis or LCMS SIM.

Aqueous Solubility. All test compounds were formulated in DMSO at a concentration of 10 mM. Reference controls were also formulated in DMSO as above. The following reference controls were used: ketoconazole, nicardipine.HCl, and tamoxifen.

Working Solutions. 50% PBS: 50% acetonitrile (Working solution A)

47.5% PBS: 47.5% acetonitrile: 5% DMSO (Working solution B)
95% PBS: 5% DMSO (Working solution C)

Solubility Test. Test compounds (12.5 μL; 10 mM) were added to PBS (237.5 μL) in quadruplicate in a 96-well plate. The wells were mixed (10 times using a 100 μL mixing volume), a coverslip was sealed on the plate, and the plate was shaken at 700 rpm at room temperature for 3 h. From each well, 250 μL was then transferred to a Merck filtration plate (Product code: MSRLN0410), and the filtration plate was placed on the Merck/Supelco vacuum manifold (Product code: 575650-U) and filtered under vacuum, and the filtrate was collected into a Merck 96-deep-well plate (product code: AXYPDW20CS). Acetonitrile (50 μL) was dispensed into a clean high-sensitivity 96-well UV−vis Corning analysis plate (Product code: CLS3635) and the aqueous filtrate (50 μL) was transferred from the collection wells to the UV analysis plate. The wells were mixed on the plate and analyzed at the λ_{max} specific to each compound. Two blanks (50 μL MeCN + 50 μL Working solution C) were included for each test compound. The results obtained were quantified against a standard calibration curve prepared for each test sample as described below.

Calibration Curve Construction. The following procedure was completed on an Apricot automatic pipettor:

Test compound (7.5 μL; 10 mM) was added in duplicate to working solution A (142.5 μL) to give a 500 μM stock concentration. This stock solution was serially diluted (4 threefold dilutions) by adding 50 μL to working solution B (100 μL) until a final concentration of 6.17 μM was achieved (5 concentrations, 6 compounds, n = 2). The stock solution was mixed 10 times with a 100 μL mix volume (or until full dissolution occurred), while each dilution was mixed five times with a 100 μL mix volume. Two blanks (Working solution B only) were included for each compound. The samples were analyzed using a BMG Labtech microplate reader first at the full spectrum (220−650 nm) of wavelengths to determine the λ_{max} specific to each compound, and then usually at the following wavelengths: 290, 300, 320, 340, 360 nm.

In Vivo **Studies.** *PK IV.* Fasted, male C57BL/6 mice were treated with an intravenous dose of **1** (nominal dose 3.00 mg/kg, administered dose 2.58 mg/kg) formulated as a 1.00 mg/mL solution in 5% DMSO, 5% solutol, and 90% water.

PK Oral. Fasted, male C57BL/6 mice were treated with a PO dose of **1** (nominal dose 10.0 mg/kg, administered dose 8.60 mg/kg) formulated as a 1.00 mg/mL solution in 5% DMSO, 5% solutol, and 90% water.

Plasma Sample Analysis.

Internal standard: 100 ng/mL Labetalol + 100

ng/mL dexamethasone + 100 ng/mL tolbutamide + 100

ng/mL verapamil + 100 ng/mL Glyburide + 100

ng/mL Celecoxib in acetonitrile

A calibration curve of **1** was established from 1 to 1000 ng/mL in male C57BL/6 mouse plasma (EDTA-K2).

An aliquot of 8 μL sample was protein-precipitated with 160 μL of IS, and the mixture was vortex-mixed well and centrifuged at 10 000 rpm for 20 min at 4 °C. The supernatant (4 μL) was injected for LC-MS/MS analysis.

◼ ASSOCIATED CONTENT

🆘 Supporting Information

The Supporting Information is available free of charge at https://pubs.acs.org/doi/10.1021/acs.jmedchem.1c01974.

> SMILES string computer-readable identifiers for the presented molecules (CSV)

> Surface plasmon resonance sensorgrams and affinity dose−response plots for **1** and **26**; LCMS chromatograms and ESI mass spectra for compounds **1**, **17**, **19**−**22**, **25**−**29**, and **32**−**47**; and molecular formula strings (PDF)

◼ AUTHOR INFORMATION

Corresponding Authors

Adrian J. Hobbs − *William Harvey Research Institute, Barts & The London School of Medicine, Queen Mary University of London, London EC1M 6BQ, U.K.*; Email: a.j.hobbs@qmul.ac.uk

David L. Selwood − *Wolfson Institute for Biomedical Research, University College London, London WC1E 6DH, U.K.*; orcid.org/0000-0002-6817-5064; Email: d.selwood@ucl.ac.uk

Authors

Robert J. Smith − *Wolfson Institute for Biomedical Research, University College London, London WC1E 6DH, U.K.*

Cristina Perez-Ternero − *William Harvey Research Institute, Barts & The London School of Medicine, Queen Mary University of London, London EC1M 6BQ, U.K.*

Daniel Conole − *Wolfson Institute for Biomedical Research, University College London, London WC1E 6DH, U.K.*; orcid.org/0000-0002-3389-8377

Capucine Martin − *William Harvey Research Institute, Barts & The London School of Medicine, Queen Mary University of London, London EC1M 6BQ, U.K.*

Samuel H. Myers − *Wolfson Institute for Biomedical Research, University College London, London WC1E 6DH, U.K.*

Complete contact information is available at:
https://pubs.acs.org/10.1021/acs.jmedchem.1c01974

Author Contributions

§R.J.S. and C.P.-T. contributed equally. All authors have given approval to the final version of the manuscript.

Notes

The authors declare no competing financial interest.

◼ ACKNOWLEDGMENTS

◼ REFERENCES

(1) Potter, L. R.; Yoder, A. R.; Flora, D. R.; Antos, L. K.; Dickey, D. M. Natriuretic peptides: their structures, receptors, physiologic functions and therapeutic applications. In *cGMP: Generators, Effectors and Therapeutic Implications*, Handbook of Experimental Pharmacology; Springer: Berlin, Heidelberg, 2009; Vol. *191*, pp 341−366.

(2) Kuhn, M. Molecular physiology of membrane guanylyl cyclase receptors. *Physiol. Rev.* **2016**, *96*, 751−804.

(3) Chinkers, M.; Garbers, D. L.; Chang, M.-S.; Lowe, D. G.; Chin, H.; Goeddel, D. V.; Schulz, S. A membrane form of guanylate cyclase is an atrial natriuretic peptide receptor. *Nature* **1989**, *338*, 78−83.

(4) Schulz, S.; Singh, S.; Bellet, R. A.; Singh, G.; Tubb, D. J.; Chin, H.; Garbers, D. L. The primary structure of a plasma membrane guanylate cyclase demonstrates diversity within this new receptor family. *Cell* **1989**, *58*, 1155−1162.

(5) Chauhan, S. D.; Nilsson, H.; Ahluwalia, A.; Hobbs, A. J. Release of C-type natriuretic peptide accounts for the biological activity of endothelium-derived hyperpolarizing factor. *Proc. Natl. Acad. Sci. U.S.A.* **2003**, *100*, 1426.

(6) Anand-Srivastava, M. B. Natriuretic peptide receptor-C signaling and regulation. *Peptides* **2005**, *26*, 1044−1059.

(7) Moyes, A. J.; Khambata, R. S.; Villar, I.; Bubb, K. J.; Baliga, R. S.; Lumsden, N. G.; Xiao, F.; Gane, P. J.; Rebstock, A.-S.; Worthington, R. J.; Simone, M. I.; Mota, F.; Rivilla, F.; Vallejo, S.; Peiró, C.; Sánchez Ferrer, C. F.; Djordjevic, S.; Caulfield, M. J.; MacAllister, R. J.; Selwood, D. L.; Ahluwalia, A.; Hobbs, A. J. Endothelial C-type natriuretic peptide maintains vascular homeostasis. *J. Clin. Invest.* **2014**, *124*, 4039−4051.

(8) Maack, T.; Suzuki, M.; Almeida, F. A.; Nussenzveig, D.; Scarborough, R. M.; McEnroe, G. A.; Lewicki, J. A. Physiological role of silent receptors of atrial natriuretic factor. *Science* **1987**, *238*, 675.

(9) Moyes, A. J.; Chu, S. M.; Aubdool, A. A.; Dukinfield, M. S.; Margulies, K. B.; Bedi, K. C., Jr.; Hodivala-Dilke, K.; Baliga, R. S.; Hobbs, A. J. C-type natriuretic peptide co-ordinates cardiac structure and function. *Eur. Heart J.* **2020**, *41*, 1006−1020.

(10) Egom, E. E.; Vella, K.; Hua, R.; Jansen, H. J.; Moghtadaei, M.; Polina, I.; Bogachev, O.; Hurnik, R.; Mackasey, M.; Rafferty, S.; Ray, G.; Rose, R. A. Impaired sinoatrial node function and increased susceptibility to atrial fibrillation in mice lacking natriuretic peptide receptor C. *J. Physiol.* **2015**, *593*, 1127−1146.

(11) Potter, L. R.; Abbey-Hosch, S.; Dickey, D. M. Natriuretic Peptides, Their Receptors, and Cyclic Guanosine Monophosphate-Dependent Signaling Functions. *Endocr. Rev.* **2006**, *27*, 47−72.

(12) Millar, J. C.; Savinainen, A.; Josiah, S.; Pang, I.-H. Effects of TAK-639, a novel topical C-type natriuretic peptide analog, on intraocular pressure and aqueous humor dynamics in mice. *Exp. Eye Res.* **2019**, *188*, No. 107763.

(13) Edelson, J. D.; Makhlina, M.; Silvester, K. R.; Vengurlekar, S. S.; Chen, X.; Zhang, J.; Koziol-White, C. J.; Cooper, P. R.; Hallam, T. J.; Hay, D. W. P.; Panettieri, R. A. In vitro and in vivo pharmacological profile of PL-3994, a novel cyclic peptide (Hept-cyclo(Cys-His-Phe-d-Ala-Gly-Arg-d-Nle-Asp-Arg-Ile-Ser-Cys)-Tyr-[Arg mimetic]-NH2) natriuretic peptide receptor-A agonist that is resistant to neutral endopeptidase and acts as a bronchodilator. *Pulm. Pharmacol. Ther.* **2013**, *26*, 229−238.

(14) Lisy, O.; Huntley, B. K.; McCormick, D. J.; Kurlansky, P. A.; Burnett, J. C. Design, synthesis, and actions of a novel chimeric natriuretic peptide: cd-nP. *J. Am. Coll. Cardiol.* **2008**, *52*, 60−68.

(15) Villar, I. C.; Panayiotou, C. M.; Sheraz, A.; Madhani, M.; Scotland, R. S.; Nobles, M.; Kemp-Harper, B.; Ahluwalia, A.; Hobbs, A. J. Definitive role for natriuretic peptide receptor-C in mediating the vasorelaxant activity of C-type natriuretic peptide and endothelium-derived hyperpolarising factor. *Cardiovasc. Res.* **2007**, *74*, 515−525.

(16) Veale, C. A.; Alford, V. C.; Aharony, D.; Banville, D. L.; Bialecki, R. A.; Brown, F. J.; Damewood, J. R.; Dantzman, C. L.; Edwards, P. D.; Jacobs, R. T.; Mauger, R. C.; Murphy, M. M.; Palmer, W. E.; Pine, K. K.; Rumsey, W. L.; Garcia-Davenport, L. E.; Shaw, A.; Steelman, G. B.; Surian, J. M.; Vacek, E. P. The discovery of non-basic

atrial natriuretic peptide clearance receptor antagonists. Part 1. *Bioorg. Med. Chem. Lett.* **2000**, *10*, 1949−1952.

(17) Namikawa, K.; Shimamoto, T.; Kitano, K.; Koyama, Y. New imidazolone compound. 2008.

(18) Iwaki, T.; Nakamura, Y.; Tanaka, T.; Ogawa, Y.; Iwamoto, O.; Okamura, Y.; Kawase, Y.; Furuya, M.; Oyama, Y.; Nagayama, T. Discovery and SAR of a novel series of Natriuretic Peptide Receptor-A (NPR-A) agonists. *Bioorg. Med. Chem. Lett.* **2017**, *27*, 4904−4907.

(19) Iwaki, T.; Oyama, Y.; Tomoo, T.; Tanaka, T.; Okamura, Y.; Sugiyama, M.; Yamaki, A.; Furuya, M. Discovery and dimeric approach of novel Natriuretic Peptide Receptor A (NPR-A) agonists. *Bioorg. Med. Chem.* **2017**, *25*, 1762−1769.

(20) Iwaki, T.; Tanaka, T.; Miyazaki, K.; Suzuki, Y.; Okamura, Y.; Yamaki, A.; Iwanami, M.; Morozumi, N.; Furuya, M.; Oyama, Y. Discovery and in vivo effects of novel human natriuretic peptide receptor A (NPR-A) agonists with improved activity for rat NPR-A. *Bioorg. Med. Chem.* **2017**, *25*, 6680−6694.

(21) Armistead, D. M.; Bemis, J. E.; Buchanan, J. L.; Dipietro, L. V.; Elbaum, D.; Geuns-Meyer, S. D.; Habgood, G. J.; Kim, J. L.; Marshall, T. L.; Novak, P. M.; Nunes, J. J.; Patel, V. F.; Toledo-Sherman, L. M.; Zhu, X. Preparation of 1,3,5-triazines as kinase inhibitors for treatment of angiogenesis or vasculogenesis. US20040116388A1, 2004.

(22) Li, Z.; Zou, H.; Zhu, W.; Shen, C.; Wang, R.; Liu, W.; Chen, X.; Tsui, H.; Yang, Z.; Zhang, X. Aminotriazines and related compounds as ErbB/BTK inhibitors and their preparation. WO2019149164A1, 2019.

(23) Likubo, K.; Kondoh, Y.; Shimada, I.; Matsuya, T.; Mori, K.; Ueno, Y.; Okada, M. Discovery of N-{2-Methoxy-4-[4-(4-methyl-piperazin-1-yl)piperidin-1-yl]phenyl}-N′[2-(propane-2-sulfonyl)-phenyl]-1,3,5-triazine-2,4-diamine (ASP3026), a potent and selective anaplastic lymphoma kinase (alk) inhibitor. *Chem. Pharm. Bull.* **2018**, *66*, 251−262.

(24) Ruehter, G.; Koch, U.; Nussbaumer, P.; Schultz-Fademrecht, C.; Eickhoff, J. Pharmaceutically active disubstituted triazine derivatives. WO2012117048A1, 2012.

(25) Venkatraj, M.; Arien, K. K.; Heeres, J.; Joossens, J.; Dirie, B.; Lyssens, S.; Michiels, J.; Cos, P.; Lewi, P. J.; Vanham, G.; Maes, L.; Van der Veken, P.; Augustyns, K. From human immunodeficiency virus non-nucleoside reverse transcriptase inhibitors to potent and selective antitrypanosomal compounds. *Bioorg. Med. Chem.* **2014**, *22*, 5241−5248.

(26) Wu, Y. Preparation of triazine derivatives as anaplastic lymphoma kinase inhibitors. CN106146478A, 2016.

(27) Marugan, J. J.; Xiao, J.; Titus, S. A.; Southall, N.; Zheng, W.; Androphy, E. J.; Cherry, J. Preparation of arylthiazolylpiperidine derivatives and analogs for use as survival motor neuron (SMN) protein production modulators. WO2011130515A1, 2011.

(28) Salituro, F.; Farmer, L.; Wang, T.; Wang, J.; Bethiel, R.; Wannamaker, M.; Martinez-Botella, G.; Duffy, J.; Aronov, A.; Lauffer, D.; Pierce, A. Deazapurines useful as inhibitors of janus kinases and their preparation, pharmaceutical compositions and use in the treatment of various diseases. WO2007041130A2, 2007.

(29) Lovett, J. A.; Portoghese, P. S. Synthesis and evaluation of melphalan-containing N,N-dialkylenkephalin analogs as irreversible antagonists of the δ opioid receptor. *J. Med. Chem.* **1987**, *30*, 1668−1674.

(30) Chen, M.-Y.; Lee, A. S.-Y. A simple and efficient esterification method. *J. Chin. Chem. Soc.* **2003**, *50*, 103−108.

(31) Conole, D.; Myers, S. H.; Mota, F.; Hobbs, A. J.; Selwood, D. L. Biophysical screening methods for extracellular domain peptide receptors, application to natriuretic peptide receptor C ligands. *Chem. Biol. Drug Des.* **2019**, *93*, 1011−1020.

(32) Thakur, M.; Thakur, A.; Khadikar, P. V.; Supuran, C. T. QSAR study on pKa vis-a-vis physiological activity of sulfonamides: a dominating role of surface tension (inverse steric parameter). *Bioorg. Med. Chem. Lett.* **2005**, *15*, 203−209.

(33) Wang, D.; Cai, Q.; Ding, K. An Efficient Copper-catalyzed amination of aryl halides by aqueous ammonia. *Adv. Synth. Catal.* **2009**, *351*, 1722−1726.

(34) Wu, X.; Hu, L. Efficient amidation from carboxylic acids and azides via selenocarboxylates: application to the coupling of amino acids and peptides with azides. *J. Org. Chem.* **2007**, *72*, 765−774.

(35) Biacore, A. B.; July, E.; Biacore, A. B. *BIAevaluation Software Handbook*, 3rd ed.; Biacore AB: Uppsala, 1997.

(36) Villar, I. C.; Bubb, K. J.; Moyes, A. J.; Steiness, E.; Gulbrandsen, T.; Levy, F. O.; Hobbs, A. J. Functional pharmacological character-ization of SER100 in cardiovascular health and disease. *Br. J. Pharmacol.* **2016**, *173*, 3386−3401.

(37) Ali, A. A. Characterization of NPRC and its binding partners. A dissertation submitted in partial fulfillment of the requirements for the degree of Doctor of Philosophy; University of South Florida: Tampa, Florida, 2009.